Published by Institute of Physics Publishing for SISSA
Received: *June 29, 2005*
Accepted: *August 9, 2005*
Published: *September 1, 2005*

Leptoquark single and pair production at LHC with CalcHEP/CompHEP in the complete model

Alexander Belyaev
Department of Physics and Astronomy
East Lansing, 48824, U.S.A.
E-mail: belyaev@pa.msu.edu.edu

Claude Leroy and Rashid Mehdiyev*
Université de Montréal, Département de Physique
Montréal, QC, H3C 3J7, Canada
E-mail: Leroy@lps.umontreal.ca, RMehdi@lps.umontreal.ca

Alexander Pukhov
Skobeltsyn Institute of Nuclear Physics, Moscow State University
Moscow 119992, Russia
E-mail: pukhov@sinp.msu.ru

Abstract: We study combined leptoquark (LQ) single and pair production at LHC at the level of detector simulation. A set of kinematical cuts to maximize significance for combined signal events has been worked out.
It was shown that combination of signatures from LQ single and pair production not only significantly increases the LHC reach, but also allows us to give the correct signal interpretation. In particular, it was found that the LHC has potential to discover LQ with a mass up to 1.2 TeV and 1.5 TeV for the case of scalar and vector LQ, respectively, and LQ single production contributes about 30-50% to the total signal rate for $LQ - l - q$ coupling, taken equal to the electromagnetic coupling.
This work is based on an implementation of the most general form of scalar and vector LQ interactions with quarks and gluons into CalcHEP/CompHEP packages. This implementation, which authors made publicly available, was one the most important aspects of the study.

Keywords: Beyond Standard Model, Phenomenological Models, Hadronic Colliders.

*On leave of absence from Institute of Physics, ANAS, Baku, AZ-370143, Azerbaijan.

JHEP09(2005)005

Contents

1. Introduction

Boson fields mediating lepton-quark interactions naturally appear in various extensions of the Standard Model which is known to be theoretically incomplete. Leptoquarks appear in the framework of Grand Unified theories (GUT) where quarks and leptons are unified in one matter multiplet [1], in the SUSY models with R-parity violation [2] (in this case the mediator of the lepton-quark interaction is a squark or a slepton), as well as in composite models of leptons and quarks [3].

In general, boson fields give rise to violation of the baryon and lepton numbers (leading to fast proton decay) and flavor changing neutral current(FCNC) processes which are strongly constrained by experiment. In principle, those bosons should be heavy ($\sim M_{\text{Planck}} \sim 10^{19}$ GeV) to suppress these unwelcome processes. On the other hand, fast proton decay and FCNC problems can be avoided if the boson mass even is of the order of the electroweak (EW) scale. In the case of leptoquarks (LQ), which exclusively induce lepton-quark interactions, the problems above are solved: 1) the fast proton decay problem is absent, since leptoquarks conserve the baryon and lepton numbers. In the case of R-parity violating SUSY, in addition to lepton-quark-squark couplings, several new interactions are possible, leading, in general, to a fast proton decay. However, the fast proton decay can be avoided as long as respective terms are set to zero, so *either* lepton *or* baryon number could be conserved; 2) the FCNC problem is also absent under the assumption of flavor diagonal form of *leptoquark-lepton-quark* ($\mathit{LQ} - l - q$) interactions.

Numerous experimental LQ searches at HERA (e.g. [4]) and at the Tevatron (for recent results see, e.g. [5] and references therein) gave no positive results so far and provided only limits on $\not{L}\!Q$ masses and $\not{L}\!Q$ couplings to leptons and quarks. Eventually, the CERN Large Hadron Collider (LHC) will be able to extend significantly the reach for $\not{L}\!Q$ masses and couplings (see, e.g. [6 − 10]). In [11 − 13] it was shown that Next-to-Leading-Order (NLO) corrections to $\not{L}\!Q$ pair production are positive and non-negligible (up to 20-40% at the Tevatron and up to 70-90% at the LHC) and lead to further extension of the collider reach in $\not{L}\!Q$ searches. Leptoquarks can be produced not only in pairs (from gluon splitting) but also as a single particle in association with lepton [14 − 16]. In [17] authors noticed the importance of the combination of $\not{L}\!Q$ single and pair production analysis for the Tevatron collider, which partially motivated the present study.

In this article, we perform a new detailed study of $\not{L}\!Q$ production and decay at LHC. There are several motivations for this work. Firstly, we stress the importance of the study of *combined* $\not{L}\!Q$ single and pair production, since both contribute to the same signature at the detector simulation level. Therefore, combination of signatures from $\not{L}\!Q$ single and pair production not only significantly increases the LHC reach, but also allows us to give the correct signal interpretation. Secondly, we study the complete set of $\not{L}\!Q$ interactions including *scalar and vector* $\not{L}\!Q$ production and decay. Finally, one should stress that this study is based on the implementation of the complete $\not{L}\!Q$ model including *the most general form of scalar and vector* $\not{L}\!Q$ *interactions with quarks and gauge bosons (including gluons)* into CalcHEP/CompHEP packages [18, 19]. This is one of the most important aspects of this work. Such an implementation allowed us to study the effect of vector $\not{L}\!Q$ interactions with gluons via anomalous couplings of the most general form.

This paper is organized as follows. In section 2, we describe the general effective lagrangian used in our study, as well as the implementation of this lagrangian into the CalcHEP/CompHEP software package. In section 3, we present signal rates for $\not{L}\!Q$ single and pair production at the LHC for the case of scalar and vector $\not{L}\!Q$. In section 4, we perform an analysis of signal versus background at the detector level. Finally, in section 5, we draw conclusions on LHC potential for leptoquarks search.

2. $\not{L}\!Q$ model and its implementation into CalcHEP/CompHEP packages

2.1 The model

Following [20, 21], we use an effective lagrangian with the most general dimensionless, SU(3) × SU(2) × U(1) invariant couplings of scalar and vector leptoquarks to leptons and quarks with lepton and baryon number conservation:

$$\mathcal{L} = \mathcal{L}^f_{|F|=0} + \mathcal{L}^f_{|F|=2} + \mathcal{L}^V \,. \tag{2.1}$$

Lagrangian $\mathcal{L}^f_{|F|=0,2}$ describes Yukawa type interactions of $\not{L}\!Q$ with leptons and quarks ($\not{L}\!Q - l - q$), changing the fermion number F by 0 or 2, respectively, where $F = 3B + L$, B is the baryon number and L is the lepton number. $\mathcal{L}^f_{|F|=0,2}$ conserves the baryon and lepton numbers and has a flavor diagonal form:

$$\begin{aligned}\mathcal{L}^f_{|F|=0} = {} & (h_{2L}\bar{u}_R\ell_L + h_{2R}\bar{q}_L i\tau_2 e_R)R_2 + \tilde{h}_{2L}\bar{d}_R\ell_L\tilde{R}_2 + (h_{1L}\bar{q}_L\ell_L + h_{1R}\bar{d}_R\gamma^\mu e_R)U_{1\mu} + \\ & + \tilde{h}_{1R}\bar{u}_R\gamma^\mu e_R\tilde{U}_{1\mu} + h_{3L}\bar{q}_L\vec{\tau}\gamma^\mu\ell_L\vec{U}_{3\mu} + \text{h.c.}\,,\end{aligned} \tag{2.2}$$

LQ(Φ)	Spin	F	Color	T_3	Q_{em}	$\lambda_L(lq)$	$\lambda_R(lq)$	$\lambda_L(\nu q)$	CalcHEP/ CompHEP notation($\Phi/\overline{\Phi}$)
S_1	0	-2	$\bar{3}$	0	$+1/3$	g_{1L}	g_{1R}	$-g_{1L}$	S1 / s1
$\tilde{S}_1$	0	-2	$\bar{3}$	0	$+4/3$	0	$\tilde{g}_{1R}$	0	ST / st
				$+1$	$+4/3$	$-\sqrt{2}g_{3L}$	0	0	SP / sp
$\vec{S}_3$	0	-2	$\bar{3}$	0	$+1/3$	$-g_{3L}$	0	$-g_{3L}$	S0 / s0
				-1	$-2/3$	0	0	$\sqrt{2}g_{3L}$	SM / sm
R_2	0	0	3	$1/2$	$+5/3$	h_{2L}	h_{2R}	0	rp / RP
				$-1/2$	$+2/3$	0	$-h_{2R}$	h_{2L}	rm / RM
$\tilde{R}_2$	0	0	3	$+1/2$	$+2/3$	$\tilde{h}_{2L}$	0	0	tp / TP
				$-1/2$	$-1/3$	0	0	$\tilde{h}_{2L}$	tm / TM
$V_{2\mu}$	1	-2	$\bar{3}$	$+1/2$	$+4/3$	g_{2L}	g_{2R}	0	VP / vp
				$-1/2$	$+1/3$	0	g_{2R}	g_{2L}	VM / vm
$\tilde{V}_{2\mu}$	1	-2	$\bar{3}$	$+1/2$	$+1/3$	$\tilde{g}_{2L}$	0	0	WP / wp
				$-1/2$	$-2/3$	0	0	$\tilde{g}_{2L}$	WM / wm
$U_{1\mu}$	1	0	3	0	$+2/3$	h_{1L}	h_{1R}	h_{1L}	u1 / U1
$\tilde{U}_{1\mu}$	1	0	3	0	$+5/3$	0	$\tilde{h}_{1R}$	0	ut / UT
				$+1$	$+5/3$	$\sqrt{2}h_{3L}$	0	0	up / UP
$\vec{U}_{3\mu}$	1	0	3	0	$+2/3$	$-h_{3L}$	0	h_{3L}	u0 / U0
				-1	$-1/3$	0	0	$\sqrt{2}h_{3L}$	um / UM

Table 1: Quantum numbers for the complete set of scalar and vector LQ fields appearing in eq. (2.2), (2.3): S_1, $\tilde{S}_1$, $\vec{S}_3$, R_2, $\tilde{R}_2$, and V_2^μ, $\tilde{V}_2^\mu$, U_1^μ, $\tilde{U}_1^\mu$, $\vec{U}_3$, respectively [21]. Also, LQ-lepton-quark couplings ($\lambda_L(lq)$, $\lambda_R(lq)$ and $\lambda_L(\nu q)$) and notation for LQ names for the model realized in CalcHEP/CompHEP are presented. The particle-antiparticle convention is defined as: $\overline{\Phi}_{F=2} \to lq$ and $\overline{\Phi}_{F=0} \to l\bar{q}$.

$$\mathcal{L}^f_{|F|=2} = (g_{1L}\bar{q}^c_L i\tau_2 \ell_L + g_{1R}\bar{u}^c_R e_R)S_1 + \tilde{g}_{1R}\bar{d}^c_R e_R \tilde{S}_1 + g_{3L}\bar{q}^c_L i\tau_2 \vec{\tau}\ell_L \vec{S}_3 + \\ + (g_{2L}\bar{d}^c_R \gamma^\mu \ell_L + g_{2R}\bar{q}^c_L \gamma^\mu e_R)V_{2\mu} + \tilde{g}_2 \bar{u}^c_R \gamma^\mu \ell_L \tilde{V}_{2\mu} + \text{h.c.}\,, \tag{2.3}$$

where τ_i are the Pauli matrices, q_L and ℓ_L are $SU(2)_L$ quark and lepton doublets, respectively and u_R, d_R, and e_R are corresponding singlet fields; charged conjugated fields are denoted by $f^c = C\bar{f}^T$. We follow the LQ classification from [21]. Table 1 summarizes the complete set of scalar and vector LQ fields appearing in eq. (2.2)–(2.3): S_1, $\tilde{S}_1$, $\vec{S}_3$, R_2, $\tilde{R}_2$, and V_2^μ, $\tilde{V}_2^\mu$, U_1^μ, $\tilde{U}_1^\mu$, $\vec{U}_3$, respectively. Scalar $(S_1, \tilde{S}_1, \vec{S}_3, R_2, \tilde{R}_2)$ and vector $(V_2^\mu, \tilde{V}_2^\mu, U_1^\mu, \tilde{U}_1^\mu, \vec{U}_3)$ LQs have Yukawa-type couplings to quarks and leptons denoted by $(g_{1(L,R)}, \tilde{g}_{1R}, g_{3L}, h_{2(L,R)}, \tilde{h}_{2L})$ and $(g_{2(L,R)}, \tilde{g}_{2R}, h_{1(L,R)}, \tilde{h}_{1R}, h_{3L})$ respectively, in eq. (2.2)–(2.3). Couplings appearing in the Feynman rules of $LQ - q - l$ ($LQ - q - \nu$) interactions (which we denote by $\lambda_L(lq)$, $\lambda_R(lq)$ and $\lambda_L(\nu q)$) are trivial linear combinations of $g, h, \tilde{g}, \tilde{h}$ couplings presented in table 1. The table also presents a notation for $I\!\!Q$ names in the model realized in CalcHEP/CompHEP packages which we describe below.

The $I\!\!Q$ interactions with gauge bosons are described by $\mathcal{L}^V$, obey the $\mathrm{SU}(3)_c\times\mathrm{SU}(2)\times \mathrm{U}(1)_Y$ Standard Model symmetry.

The $I\!\!Q$ − *gluon* interactions are described by the lagrangian of the most general form [22] for the scalar and vector $I\!\!Q$ interactions, $\mathcal{L}^g_S$ and $\mathcal{L}^g_V$, respectively:

$$\mathcal{L}^g_S = \sum_{\text{scalars}} \left[\left(D^{\mu}_{ij}\Phi^j\right)^{\dagger} \left(D^{ik}_{\mu}\Phi_k\right) - M_S^2 \Phi^{i\dagger}\Phi_i \right], \tag{2.4}$$

$$\mathcal{L}^g_V = \sum_{\text{vectors}} \left\{ -\frac{1}{2} V^{i\dagger}_{\mu\nu}V^{\mu\nu}_i + M_V^2 \Phi^{i\dagger}_{\mu}\Phi^{\mu}_i - ig_s \left[(1-\kappa_G)\Phi^{i\dagger}_{\mu} t^a_{ij}\Phi^j_{\nu}\mathcal{G}^{\mu\nu}_a + \frac{\lambda_G}{M_V^2} V^{i\dagger}_{\sigma\mu} t^a_{ij} V^{j\mu}_{\nu}\mathcal{G}^{\nu\sigma}_a \right] \right\}. \tag{2.5}$$

Here, g_s denotes the strong coupling constant, t_a are the generators of $\mathrm{SU}(3)_c$, $M_S(M_V)$ are the scalar(vector) leptoquark masses, while κ_G and λ_G are the anomalous couplings related to the anomalous magnetic and quadrupole moments of vector $I\!\!Q$ [22]. Fields Φ and Φ^{μ} represent scalar and vector leptoquarks, respectively. The field strength tensors of the gluon and vector leptoquark fields are:

$$\begin{aligned} \mathcal{G}^a_{\mu\nu} &= \partial_{\mu}G^a_{\nu} - \partial_{\nu}G^a_{\mu} + g_s f^{abc}G_{\mu b}G_{\nu c}, \\ V^i_{\mu\nu} &= D^{ik}_{\mu}\Phi_{\nu k} - D^{ik}_{\nu}\Phi_{\mu k}\,, \end{aligned} \tag{2.6}$$

with the covariant derivative given by

$$D^{ij}_{\mu} = \partial_{\mu}\delta^{ij} - ig_s t^{ij}_a G^a_{\mu}\,. \tag{2.7}$$

We omit here the analogous $\mathrm{U}(1)_Y\times\mathrm{SU}(2)$ piece of gauge interactions since it is not relevant for our study of $I\!\!Q$ production at LHC, where (gauge boson — $I\!\!Q$) interactions are eventually gluon-dominated.

We would like to stress that the $I\!\!Q$ study in this paper is restricted to interactions of eq. (2.1). Similar study, in the SUSY framework, for example, are expected to be qualitatively different, in general, unless interactions are dominated by R-parity violating interactions.

2.2 $I\!\!Q$ color factorization and model implementation into CalcHEP/CompHEP

The appearance of vertex with 4 color particles can not be straightforwardly implemented into CalcHEP/CompHEP packages. The idea is to split 4-color interactions into 3-color vertices via the introduction of auxiliary ghosts fields.

It is well known that for $G\bar{q}q$ and GGG QCD vertices their color structure is factorisable. For calculation of Feynman diagrams with such vertices, where color indexes can be convolved separately, an elegant technique is presented in [23]. However, for $4G$ vertex such a factorization is absent. To have color factorization in the case of $4G$ vertex one can

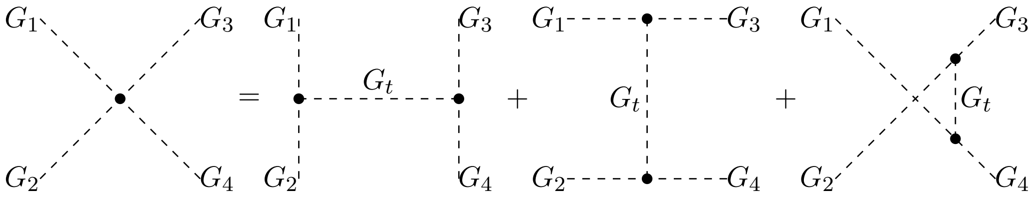

Figure 1: Splitting of a four-gluon vertex into three-gluon vertex.

split this vertex into $3G$ vertex by means of the auxiliary tensor field $G_{t\mu\nu}$ [19]. This field should have the point-like propagator

$$\langle 0|T[G_{t\alpha_1}^{\mu_1\nu_1}(p_1),\ G_{t\alpha_2}^{\mu_2\nu_2}(p_2)]|0\rangle = \frac{1}{(2\pi)^4 i}\,\delta(p_1+p_2)\,\delta_{\alpha_1\alpha_2} g^{\mu_1\mu_2}\,g^{\nu_1\nu_2}\,. \tag{2.8}$$

and interact with gluons according to

$$S_{G_tGG} = \frac{i\,g}{\sqrt{2}}\int f^{\alpha}_{\beta\gamma} G_{t\alpha}{}^{\mu\nu}(x) G^{\beta}_{\mu}(x) G^{\gamma}_{\nu}(x) d^4x\,. \tag{2.9}$$

Graphically, it can be represented as in figure 1.

This trick was successfully implemented in CompHEP/CalcHEP packages for QCD lagrangian. However in the case of the interaction of vector leptoquarks with gluon [22] one needs to develop this technique further and find a general prescription for splitting of the arbitrary color structure. Such a prescription is described below. We consider separately cases of real (e.g. gluon) and complex (e.g. leptoquark) vector fields.

In the case of a *real vector field* Φ_μ interacting with a gluon field G_μ, the lagrangian can be presented as

$$L = -\frac{1}{4}|\partial_\mu\Phi_\nu - \partial_\nu\Phi_\mu + \Upsilon_{\mu\nu}|^2 + \mathrm{Int}(\Upsilon(\Phi,G),\Phi,\ldots)\,, \tag{2.10}$$

where $\Upsilon_{\mu\nu} = g[\Phi_\mu, G_\nu]$, Int represents terms of gluon interaction with color matter realized via general derivative or the strength tensor $F_{\mu\nu}$. The color index of the gluon fields is omitted to simplify the expressions.

Now, we replace $\Upsilon_{\mu\nu}$ by an auxiliary field $T_{\mu\nu}$ and confine of $\Upsilon = T$ by means of a Lagrange multiplier $t^{\mu\nu}$. We apply this procedure for the Int and $\Upsilon(\Phi,G)^2$ terms, keeping the linear Υ term as it is:

$$\begin{aligned} L = &-\frac{1}{4}|\partial_\mu\Phi_\nu - \partial_\nu\Phi_\mu|^2 - \frac{1}{2}(\partial_\mu\Phi_\nu - \partial_\nu\Phi_\mu)\Upsilon(\Phi,G)^{\mu\nu} - \\ &-\frac{1}{4}T_{\mu\nu}T^{\mu\nu} + \frac{1}{2}t_{\mu\nu}(T^{\mu\nu} - \Upsilon(\Phi,G)^{\mu\nu}) + \mathrm{Int}(\Upsilon\to X,\Phi,\ldots)\,. \end{aligned} \tag{2.11}$$

Then, we perform the following substitution of variables

$$\Phi_{T\mu\nu} = \frac{(T_{\mu\nu} - t_{\mu\nu})}{\sqrt{2}} \qquad \text{and} \qquad \Phi_{t\mu\nu} = i\cdot\frac{t_{\mu\nu}}{\sqrt{2}} \tag{2.12}$$

in order to obtain standard normalized quadratic forms for the auxiliary fields:

$$\begin{aligned} L = &-\frac{1}{4}|\partial_\mu\Phi_\nu - \partial_\nu\Phi_\mu|^2 - \frac{1}{2}(\partial_\mu\Phi_\nu - \partial_\nu G_\mu)\Upsilon(\Phi,G)^{\mu\nu} - \\ &- \frac{1}{2}\Phi_{T\mu\nu}\Phi_T{}^{\mu\nu} - \frac{1}{2}\Phi_{t\mu\nu}\Phi_t{}^{\mu\nu} + \frac{i}{\sqrt{2}}\Phi_t\Upsilon(\Phi,G)^{\mu\nu} + \\ &+ \mathrm{Int}(\Upsilon \to \sqrt{2}(\Phi_T - i\cdot\Phi_t), G, \ldots)\,. \end{aligned} \tag{2.13}$$

In the case of QCD interaction with scalar and fermion fields, the $Int()$ term does not contain Υ. Thus, the auxiliary field T is free and can be omitted. Other terms produce the $3-gluon$ interaction, the point-like propagator (2.8), and the interaction of *just one* auxiliary tensor field t with gluons (2.9).

Lagrangian with a *complex vector* field Φ also can be represented in a color-factored form using the same trick. In a general case, it is given as:

$$L = -\frac{1}{2}|\partial_\mu\Phi_\nu - \partial_\nu\Phi_\mu + \Upsilon(\Phi,G)_{\mu\nu}|^2 + \mathrm{Int}(\Upsilon(\Phi,G),\Upsilon(\Phi,G)^*,\Phi,\Phi^*,\ldots)\,. \tag{2.14}$$

Following the procedure adopted with real vector field, we introduce two auxiliary fields $T_{\mu\nu}$ and $t_{\mu\nu}$ which are now complex. In terms of these fields, the lagrangian becomes:

$$\begin{aligned} L = &-\frac{1}{2}|\partial_\mu\Phi_\nu - \partial_\nu\Phi_\mu|^2 - \frac{1}{2}(\partial_\mu\Phi^*_\nu - \partial_\nu\Phi^*_\mu)\Upsilon(\Phi,G)^{\mu\nu} - \frac{1}{2}\Upsilon(\Phi,G)^*_{\mu\nu}(\partial^\mu V^\nu - \partial^\nu V^\mu) - \\ &- \frac{1}{2}T^*_{\mu\nu}T^{\mu\nu} + \frac{1}{2}t^*_{\mu\nu}(T^{\mu\nu} - \Upsilon(\Phi,G)^{\mu\nu}) + \frac{1}{2}(T^*_{\mu\nu} - \Upsilon(\Phi,G)^*_{\mu\nu})t^{\mu\nu} + \\ &+ \mathrm{Int}(\Upsilon \to T, \Upsilon(\Phi,G)^* \to T^* \ldots)\,. \end{aligned} \tag{2.15}$$

To obtain a standard normalized quadratic form of auxiliary fields, one should perform the following variable substitutions:

$$\begin{aligned} \Phi_{T\mu\nu} &= \frac{(T_{\mu\nu} - t_{\mu\nu})}{\sqrt{2}}, & \Phi_{T^*_{\mu\nu}} &= \frac{(T^*_{\mu\nu} - t^*_{\mu\nu})}{\sqrt{2}} \\ \Phi_{t\mu\nu} &= i\cdot\frac{t_{\mu\nu}}{\sqrt{2}}, & \Phi_{t^*_{\mu\nu}} &= i\cdot\frac{t^*_{\mu\nu}}{\sqrt{2}}; \end{aligned} \tag{2.16}$$

Note that the second line realizes a *non-analytic* parameter substitution, which, in general, is legal for functional integrals. Now, the lagrangian in color-factorized form can be given as

$$\begin{aligned} L = &-\frac{1}{2}|\partial_\mu\Phi_\nu - \partial_\nu\Phi_\mu|^2 - \frac{1}{2}(\partial_\mu\Phi^*_\nu - \partial_\nu\Phi^*_\mu)\Upsilon(\Phi,G)^{\mu\nu} - \frac{1}{2}\Upsilon(\Phi,G)^*_{\mu\nu}(\partial^\mu\Phi^\nu - \partial^\nu\Phi^\mu) - \\ &- |\Phi_T|^2 - |\Phi_t|^2 + \frac{i}{\sqrt{2}}\Phi_{t^*_{\mu\nu}}\Upsilon(\Phi,G)^{\mu\nu} + \frac{i}{\sqrt{2}}\Upsilon(\Phi,G)^*_{\mu\nu}\Phi_t{}^{\mu\nu} \\ &+ \mathrm{Int}(\Upsilon \to \sqrt{2}(\Phi_T - i\cdot\Phi_t), \Upsilon(\Phi,G)^* \to \sqrt{2}(\Phi^*_T - i\cdot\Phi^*_t)\ldots)\,. \end{aligned} \tag{2.17}$$

In particular, for the case of lagrangian (2.5) one has

$$\Upsilon(\Phi,G)_{\mu\nu} = -ig(G_\mu\Phi_\nu - G_\nu\Phi_\mu) \tag{2.18}$$

$$\Upsilon(\Phi,G)^*_{\mu\nu} = ig(G_\mu\Phi^\dagger_\nu - G_\nu\Phi^\dagger_\mu) \tag{2.19}$$

$$\begin{aligned}&\mathrm{Int}(\Upsilon \to \sqrt{2}(\Phi_T - i\cdot\Phi_t), \Upsilon(\Phi,G)^* \to \sqrt{2}(\Phi_T^* - i\cdot\Phi_t^*)\ldots) =\\
&\quad = -ig(1-\kappa_G)\Phi_\mu t^a \Phi_\nu[\partial_\mu G^a_\nu - \partial_\nu G^a_\mu + \sqrt{2}(\Phi_{t}{}^a_{\mu\nu} - i\Phi_{T}{}^a_{\mu\nu})] -\\
&\quad - ig\frac{\lambda_G}{M_\Phi^2}[\partial_\sigma \Phi^\dagger{}_\mu - \partial_\mu\Phi^\dagger{}_\sigma + \sqrt{2}(\Phi_{T}{}^*_{\sigma\mu} - i\Phi_{t}{}^*_{\sigma\mu})] \times\\
&\quad \times [\partial_\nu\Phi^\mu - \partial^\mu\Phi_\nu + \sqrt{2}(\Phi_{T}{}^\mu_\nu - i\Phi_{t}{}^\mu_\nu)] \times [(\partial^\nu G^\sigma - \partial^\sigma G^\nu + \sqrt{2}(G_T{}^{\nu\sigma} - iG_t{}^{\nu\sigma})]\,.\end{aligned} \tag{2.20}$$

In the case of a *complex scalar* field one should introduce two auxiliary *vector* fields — V_μ and v_μ (analogous to $T_{\mu\nu}$ and $t_{\mu\nu}$ tensors). The lagrangian with the complex scalar field Φ can be represented as:

$$L = |\partial_\mu\Phi + \Upsilon(\Phi,G)_\mu|^2 + \mathrm{Int}(\Upsilon(\Phi,G), \Upsilon(\Phi,G)^*, \Phi, \Phi^*, \ldots)\,. \tag{2.21}$$

In terms of these fields, in exact analogy with the vector leptoquark field, we have

$$\begin{aligned} L =\ & |\partial_\mu\Phi|^2 + \partial_\mu\Phi^*\Upsilon(\Phi,G)^\mu + \Upsilon(\Phi,G)^*_\mu\partial^\mu\Phi +\\
& + V^*_\mu V^\mu - v^*_\mu[V^\mu - \Upsilon(\Phi,G)^\mu] - [V^*_\mu - \Upsilon(\Phi,G)^*_\mu]v^\mu +\\
& + \mathrm{Int}(\Upsilon \to V, \Upsilon(\Phi,G)^* \to V^*\ldots)\end{aligned} \tag{2.22}$$

with the same variable substitutions:

$$\begin{aligned}\Phi_{V\mu} &= \frac{(V_\mu - v_\mu)}{\sqrt{2}} & \Phi_{V}{}^*_\mu &= \frac{(V^*_\mu - v^*_\mu)}{\sqrt{2}}\\
\Phi_{v\mu} &= i\cdot\frac{v_\mu}{\sqrt{2}} & \Phi^*_{v\mu} &= i\cdot\frac{v^*_\mu}{\sqrt{2}}\,.\end{aligned} \tag{2.23}$$

Here, like in eq. (2.16), the parameter substitution is a non-analitic one. For lagrangian (2.4) one has:

$$\Upsilon(\Phi,G)_\mu = -igG_\mu\Phi \tag{2.24}$$

$$\Upsilon(\Phi,G)^*_\mu = igG_\mu\Phi \tag{2.25}$$

$$\mathrm{Int}(\Upsilon \to \sqrt{2}(\Phi_V - i\cdot\Phi_v), \Upsilon(\Phi,G)^* \to \sqrt{2}(\Phi_V^* - i\cdot\Phi_v^*)\ldots) = 0\,. \tag{2.26}$$

One can see that the leptoquark lagrangians given by eq. (2.4)–(2.5) can be rewritten in terms of products of only three fields. The approach described above allows us to represent the strength tensor as a sum of vector fields and auxiliary tensor fields. Thus, interactions can be presented as a trilinear fields interaction only and, therefore, have simple unambiguously defined color factor that can be factorized.

As it was demonstrated above, the implementation of the complete LQ model requires *two* auxiliary tensor fields $\Phi.t$ and $\Phi.T$ for each LQ type. In CompHEP [19], only one tensor field ($\Phi.t$) is automatically generated, while CalcHEP [18] generates both of them. To implement the complete LQ model into CompHEP one can introduce the second tensor field by doubling the vector LQ fields (by introducing, say, $\tilde\Phi$ LQ fields), and use the tensor field of those particles ($\tilde\Phi.t$) as a $\Phi.T$ field. The complete LQ model given by eq. (2.2)–(2.5) has been implemented and tested for both CompHEP and CalcHEP packages. The complete models of LQ interactions relevant to LHC or Tevatron physics (i.e. models with

JHEP09(2005)005

```
P1   |P2   |P3   |  Factor              | Lorentz Part
------------------------------------------------------------------------------------------
vm   |VM   |G    |  GG/MVM^2            |MVM^2*((1-KG)*(m2.p3*m1.m3-m1.p3*m2.m3)
                                        |     +(p2.m1*m2.m3-p1.m2*m1.m3+(p1-p2).m3*m1.m2))
                                        |      +LG*( p3.m1*(p1.m2*p2.m3-p1.p2*m2.m3)
                                        |           -p3.m2*(p1.m3*p2.m1-p1.p2*m1.m3)
                                        |           +p2.p3*(p1.m3*m1.m2-p1.m2*m1.m3)
                                        |          -p1.p3*(p2.m3*m1.m2-p2.m1*m2.m3))
vm   |VM.t |G    |  GG/MVM^2/Sqrt2      |MVM^2*( m1.m2*m3.M2-m1.M2*m3.m2)
                                        |+2*LG*( p3.m2*(p1.m3*m1.M2-p1.M2*m1.m3)
                                        |       +m3.m2*(p1.M2*p3.m1-p1.p3*m1.M2))
VM   |vm.t |G    | -GG/MVM^2/Sqrt2      |MVM^2*(m1.m2*m3.M2-m1.M2*m3.m2)
                                        |+2*LG*( p3.m2*(p1.m3*m1.M2-p1.M2*m1.m3)
                                        |        +m3.m2*(p1.M2*p3.m1-p1.p3*m1.M2))
vm   |VM.T |G    | i*GG/MVM^2*Sqrt2     |LG*( p3.m2*(p1.m3*m1.M2-p1.M2*m1.m3)
                                        |    +m3.m2*(p1.M2*p3.m1-p1.p3*m1.M2))
VM   |vm.T |G    |-i*GG/MVM^2*Sqrt2     |LG*( p3.m2*(p1.m3*m1.M2-p1.M2*m1.m3)
                                        |     +m3.m2*(p1.M2*p3.m1-p1.p3*m1.M2))
vm   |VM   |G.t  |  -GG*Sqrt2/MVM^2     |MVM^2*(1-KG)*m1.m3*m2.M3
                                        |-LG*( p1.M3*m1.m2*p2.m3-p1.m2*p2.m3*m1.M3
                                        |     -p1.M3*m2.m3*p2.m1+p1.p2*m1.M3*m2.m3)
vm   |VM   |G.T  |-i*GG*Sqrt2/MVM^2     |MVM^2*(1-KG)*m1.m3*m2.M3
                                        |-LG*( p1.M3*m1.m2*p2.m3-p1.m2*p2.m3*m1.M3
                                        |     -p1.M3*m2.m3*p2.m1+p1.p2*m1.M3*m2.m3)
vm   |VM.t |G.t  |   2*GG*LG/MVM^2      |m2.m3*(p1.M3*m1.M2-p1.M2*m1.M3)
vm   |VM.t |G.T  | 2*i*GG*LG/MVM^2      |m2.m3*(p1.M3*m1.M2-p1.M2*m1.M3)
vm   |VM.T |G.t  | 2*i*GG*LG/MVM^2      |m2.m3*(p1.M3*m1.M2-p1.M2*m1.M3)
vm   |VM.T |G.T  |  -2*GG*LG/MVM^2      |m2.m3*(p1.M3*m1.M2-p1.M2*m1.M3)
VM   |vm.t |G.t  |   2*GG*LG/MVM^2      |m2.M3*(p1.m3*m1.M2-p1.M2*m1.m3)
VM   |vm.t |G.T  | 2*i*GG*LG/MVM^2      |m2.M3*(p1.m3*m1.M2-p1.M2*m1.m3)
VM   |vm.T |G.t  | 2*i*GG*LG/MVM^2      |m2.M3*(p1.m3*m1.M2-p1.M2*m1.m3)
VM   |vm.T |G.T  |  -2*GG*LG/MVM^2      |m2.M3*(p1.m3*m1.M2-p1.M2*m1.m3)
vm.T |VM.T |G.T  |-i*GG*LG/MVM^2*2*Sqrt2| m1.M3*M1.M2*m2.m3
vm.t |VM.T |G.T  |  -GG*LG/MVM^2*2*Sqrt2| m1.M3*M1.M2*m2.m3
vm.T | VM.t|G.T  |  -GG*LG/MVM^2*2*Sqrt2| m1.M3*M1.M2*m2.m3
vm.t | VM.t|G.T  | i*GG*LG/MVM^2*2*Sqrt2| m1.M3*M1.M2*m2.m3
vm.T |VM.T |G.t  |  -GG*LG/MVM^2*2*Sqrt2| m1.M3*M1.M2*m2.m3
vm.t |VM.T |G.t  | i*GG*LG/MVM^2*2*Sqrt2| m1.M3*M1.M2*m2.m3
vm.T | VM.t|G.t  | i*GG*LG/MVM^2*2*Sqrt2| m1.M3*M1.M2*m2.m3
vm.t | VM.t|G.t  |   GG*LG/MVM^2*2*Sqrt2| m1.M3*M1.M2*m2.m3
vm.t | VM.t|G    | 2*GG*LG/MVM^2        | M1.M2*(p3.m2*m1.m3-p3.m1*m2.m3)
vm.T | VM.t|G    |2*i*GG*LG/MVM^2       | M1.M2*(p3.m2*m1.m3-p3.m1*m2.m3)
vm.t |VM.T |G    |2*i*GG*LG/MVM^2       | M1.M2*(p3.m2*m1.m3-p3.m1*m2.m3)
vm.T |VM.T |G    | -2*GG*LG/MVM^2       | M1.M2*(p3.m2*m1.m3-p3.m1*m2.m3)
```

Table 2: An example of the implementation of LQ interactions with gluons in the CalcHEP/CompHEP packages for the case of $V_{2\mu}$ vector LQ (VM) with $F=-2, T_3=-1/2, Q=+1/3$. See text for details.

$LQ-l-q$ and $LQ-gluon$ interactions) can be found here [24]. Results for LQ pair production has been compared with those of paper [22]. We agree with the results of [22] except with the sign in front of λ_G in the expression for vector LQ pair production (for the sign convention defined by eq. (2.5)), which we found to be opposite in our calculations.

In table 2, we present an explicit example of the implementation of LQ interactions with gluons in the CalcHEP package for the case of $V_{2\mu}$ vector LQ (VM) with $F = -2, T_3 = -1/2, Q = +1/3$ (see table 1). Table 2 is a piece of the CalcHEP model of particle interactions. The first three fields '$P1$', '$P2$' and '$P3$' include the names of the interacting particles. The last two fields 'Factor' and 'Lorentz Part' define a vertex itself. Each line of the table represents a particles interaction vertex. Symbols 'up', 'up.t','up.T' correspond to a vector LQ, first tensor LQ and second tensor LQ fields, respectively. Names with capital letters: 'UP', 'UP.t','UP.T' correspond to the hermitean conjugated fields. Gluon fields and its two tensor fields are denoted by 'G','G.t','G.T', respectively. The 'Factor' field contains 'GG', 'MUP', 'LG' and 'Sqrt2' which denote g_s, M_{UP} (LQ mass), λ_G and $\sqrt{2}$, respectively. Symbols '$mi.mj$', '$Mi.mj$', '$mi.Mj$' or '$Mi.Mj$' ($i, j = 1, ...3$) in 'Lorentz Part' stand for $g^{m_i m_j}$, $g^{M_i m_j}$, $g^{m_i M_j}$ or $g^{M_i M_j}$ metric tensors, respectively, with the indices folded with the respective index of vector or tensor particle in the column 'i' and 'j'. The first index of the tensor particle is denoted by a lower case letter, e.g., '$m1$', while the second index — by a capital letter, e.g. '$M1$'. The index of the vector particle is always a lower case letter, e.g. '$m1$'. The symbols '$pi.mj$' or '$pi.Mj$' denote '$p_i^{m_j}$' and '$p_i^{M_j}$' i.e. the momenta of the interacting particles with the respective Lorentz indices. The symbols '$pi.pj$' denote the momenta product, $p_i.p_j$, of two particles. The symbol 'KG' in the 'Lorentz Part' denotes the anomalous coupling κ_G. A detailed explanation on the implementation of models of particle interactions can be found in the CompHEP manual [19].

3. Signal rates

Leptoquarks can be produced in quark-quark, quark-gluon and gluon-gluon interactions. Their production at the LHC is dominated by the strong interaction of LQ with gluons, and one can safely neglect LQ interactions with photons, Z and $W^{\pm}$ bosons. In the case of quark-quark and gluon-gluon fusion, LQ produced *in pairs* are shown by Feynman diagrams in figure 2. The LQ pair production cross section is defined by LQ mass and coupling of the strong interactions — α_s. In the case of *vector* LQ pair production the total cross section also depends on the anomalous κ_G and λ_G couplings.

In the case of quark-gluon fusion, LQ are produced *singly* in association with leptons. In comparison to LQ pair production, the production rate of LQ single rate depends also on

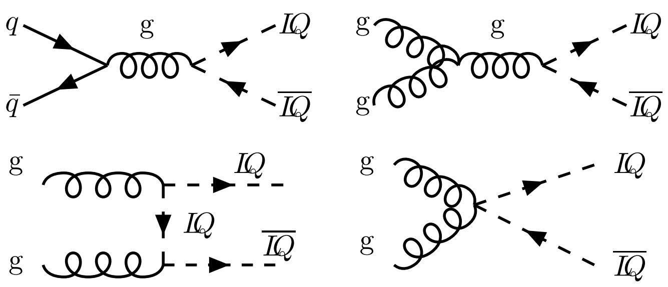

Figure 2: Diagrams for LQ pair production in quark-quark and gluon-gluon fusion.

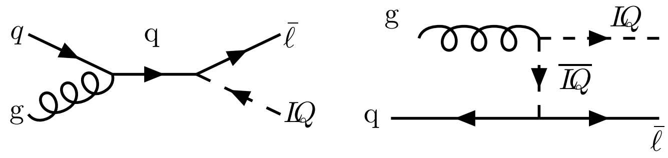

Figure 3: Diagrams for IQ single production in quark-gluon fusion

IQ $-$ *quark* $-$ *lepton* Yukawa type coupling appearing in eq. (2.2)–(2.3). The corresponding diagrams are shown in figure 3.

Both processes — IQ single and pair production — give the same striking signatures:

1. $2l + jets$ when IQs decay into a lepton and a quark;

2. $l + jets + \not{E}_T$ for both processes when singly produced IQ decays into a neutrino and a quark and one of the IQ produced in pair production, decays into a lepton and a quark while the other decays into a neutrino and a quark. The same signature will take place for IQ single production if IQ is produced in association with a neutrino but decays into a lepton and a quark.

3. $jets + \not{E}_T$ signature when IQs decay into a neutrino and a quark and single IQ is produced in association with a neutrino.

One of the important message which we would like to convey in this article is that IQ single and pair productions must be considered together. Because of similarity in their signatures, it is impossible to separate signals from IQ single and pair production completely.

In our study, for numerical calculations we have used the CTEQ6L set for parton distribution function (PDF) [27] and chosen the QCD scale equal to the IQ mass. There are many scalar and vector IQ species with different isospin, charge and IQ $-$ *quark* $-$ *lepton* couplings (as given in table 1), however, the total IQ decay width depends on one parameter (given that IQ mass and α_S are fixed), the sum of IQ $-$ *quark* $-$ *lepton* couplings squared, $\lambda^2_{\rm eff} = \lambda^2_L(lq) + \lambda^2_R(lq) + \lambda^2_L(\nu q')$ (see table 1 and eq. (2.2), (2.3). Without loosing generality, for our analysis, we have chosen scalar($S0$) and vector(VM) IQ (see table 1), which couples to both — the charged lepton and a quark as well as to a neutrino and a quark. For the reference point, we have chosen $\lambda_{\rm eff}$ to be equal to the electromagnetic coupling, $e = \sqrt{4\pi\alpha} \simeq 0.312$ for $\alpha = 1/128$. Choosing $\lambda_{\rm eff}$ completely defines IQ decay width:

$$S0 \text{ with } F = -2\,,\ T_3 = 0\,,\ Q = +\frac{1}{3} \text{ has } \Gamma = M_{IQ}\frac{(\lambda^2_L(lq) + \lambda^2_L(\nu q'))}{16\pi}\,, \tag{3.1}$$

$$\text{while } VM \text{ with } F = -2\,,\ T_3 = -\frac{1}{2}\,,\ Q = +\frac{1}{3} \text{ has } \Gamma = M_{IQ}\frac{(\lambda^2_R(lq) + \lambda^2_L(\nu q')}{24\pi}\,. \tag{3.2}$$

Both, $S0$ and VM, decay into $\bar{u}e^+$ and $\bar{d}\bar{\nu}$ with 50% branching fraction for each decay channel for our choice of parameters. For $M_{IQ} = 1\,\text{TeV}$, $\sqrt{g^2_{3L} + g^2_{3L}} = \sqrt{g^2_{2R} + g^2_{2L}} = \lambda_{\rm eff} = e$, the total width for $S0$ is $\Gamma(S0) = 1.95\,\text{GeV}$ while $\Gamma(VM) = 1.30\,\text{GeV}$.

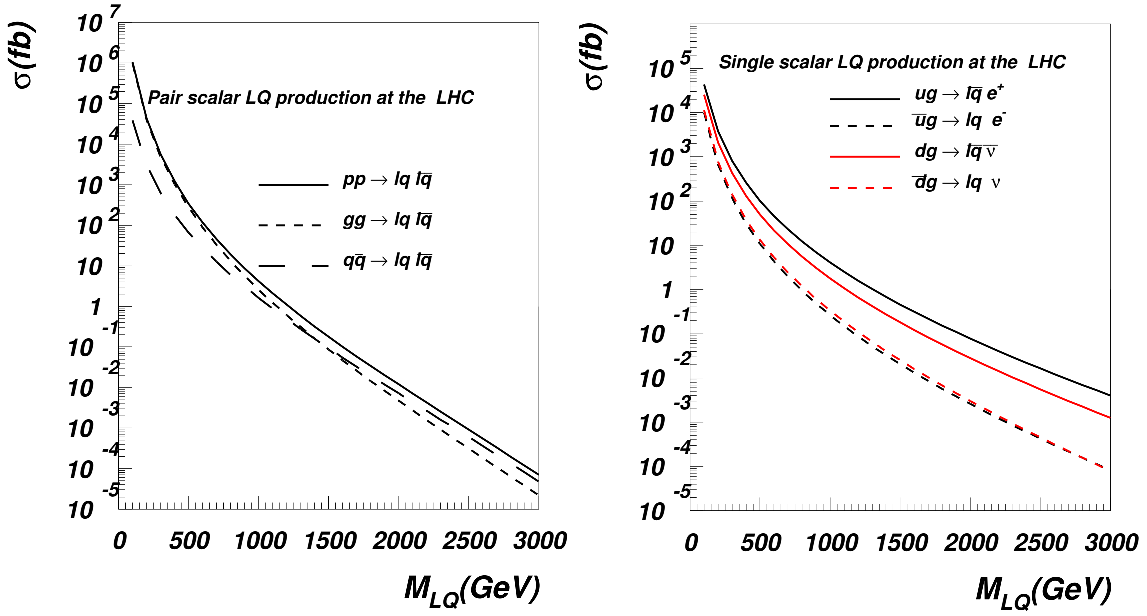

Figure 4: Total cross section of scalar LQ (S_0) production as a function of the LQ mass for LQ pair (left) and single (right) production at the LHC. The cross section of single LQ production depends on the value LQ $-\,\ell\,-\,q$ coupling chosen to be $\sqrt{g_{3L}^2 + g_{3L}^2} = \lambda_{\rm eff} = e$. The single LQ production in association with charged lepton is represented by black curves while its production in association with neutrino is shown by red curves.

In figure 4 we present the total cross section of scalar LQ production as a function of LQ mass for LQ pair (left) and single (right) production. One should note, that single LQ and single $\overline{\rm LQ}$ production rates at the LHC are drastically different since the first of them is initiated by valence quarks while the other one – by sea quarks. Below, we quote the sum of the cross sections for LQ and $\overline{\rm LQ}$ single production. LQ single production rates also depend on to which quark(s) it couples. In figure 4 one can see the difference in rates for single LQ production when it is produced in association with charged lepton (higher rates) and when it is produced in association with a neutrino (lower rates). The apparent origin of this difference lies in the difference between *up*− and *down*− quark parton densities, respectively. We do not lose generality when studying just one type of scalar LQ, $S0$ here, since the generic cross section of the scalar LQ single production could be expressed as a superposition of two cross sections represented by the red and black curves in figure 4 which scales quadratically with the LQ $- l - q$ coupling. The same is also true for the case of vector LQ production which we describe below.

For low LQ masses ($\sim$ 100 GeV) LQ pair production process dominates over the LQ single production process by about one order of magnitude: $\sim$ 1000 pb compared with $\sim$ 100 pb. But for larger LQ masses ($\sim$ 1000 GeV), targeted by LHC (unless Tevatron will discover light LQ states earlier) the cross sections of LQ single and pair production become comparable. This happens because of a stronger phase space suppression of LQ pair production and a related faster drop of the parton (especially gluon) density functions. For $M_{LQ} \sim 1000$ GeV, the cross section for both, single and LQ pair production, is roughly of the order of 10 fb. For even higher scalar LQ masses, single production starts to dominate over

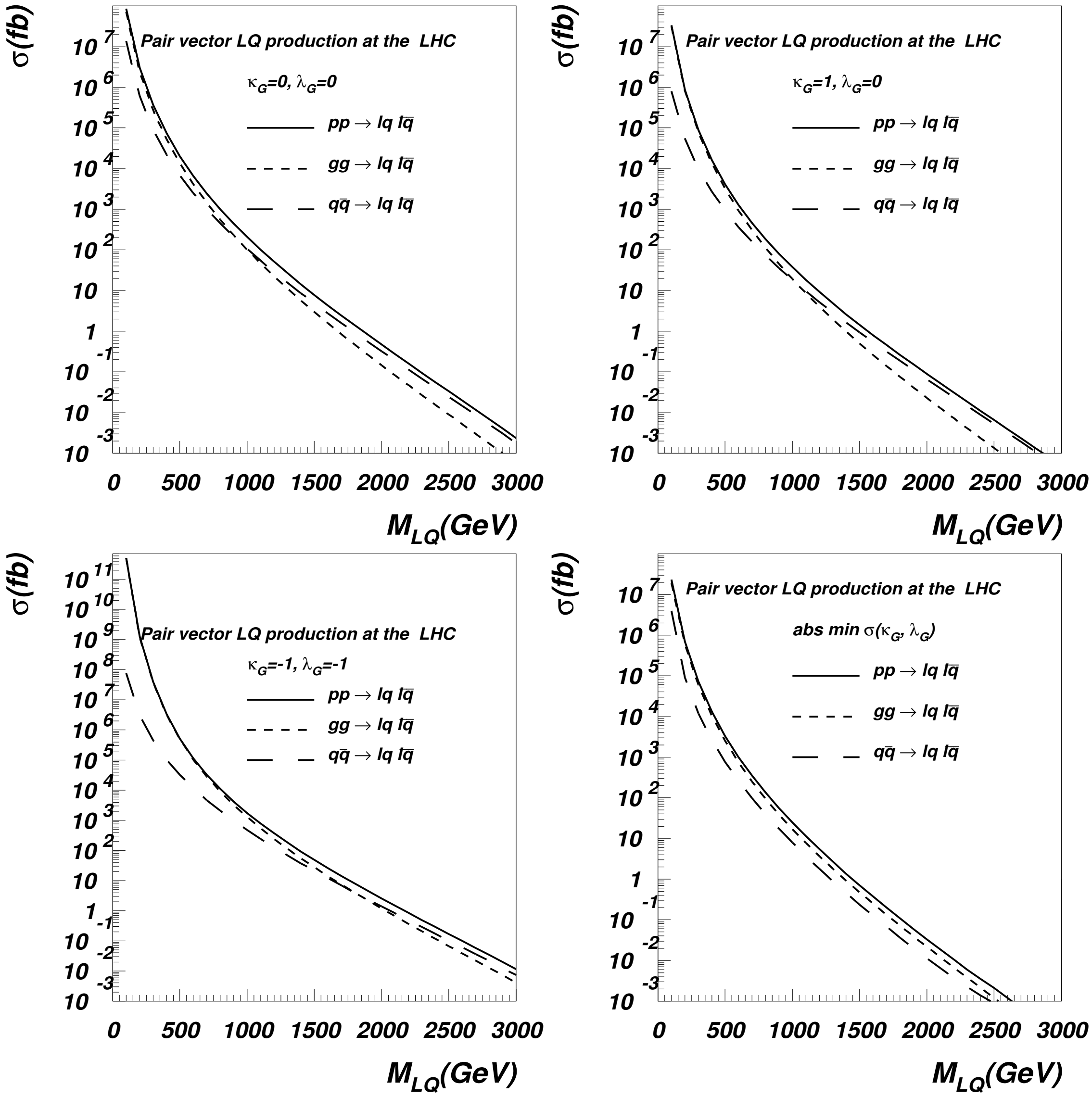

Figure 5: Total cross section for pair vector LQ production as a function of the LQ mass. Four choices of (κ, λ) are presented: 1) $\kappa_G = \lambda_G = 0$ — Yang-Mills type coupling (YM); 2) $\kappa_G = 1$, $\lambda_G = 0$ — Minimal coupling (MC); 3) $\kappa_G = -1$, $\lambda_G = -1$ — (MM) and 4) the case of *absolute minimal cross section* (AM) in which the cross-section is minimized with respect to κ_G, λ_G parameters for each value of M_{LQ}.

LQ pair production — for $M_{LQ} \sim 2000\,\mathrm{GeV}$, the LQ single production cross section ($\sim 0.1\,\mathrm{fb}$) is already one order of magnitude larger than the cross section of pair LQ production ($\sim 0.01\,\mathrm{fb}$)! Of course, the cross section of LQ single production is proportional to the square of the $LQ - e - q$ unknown coupling (chosen to be equal to the electromagnetic coupling) and can be rescaled accordingly. One can see that if this coupling is of the order of the electromagnetic coupling, then the scalar LQ single production should be definitely taken into account and combined with the studies of the LQ pair production. This region of coupling has been probed with the recent experimental limits obtained at HERA [4].

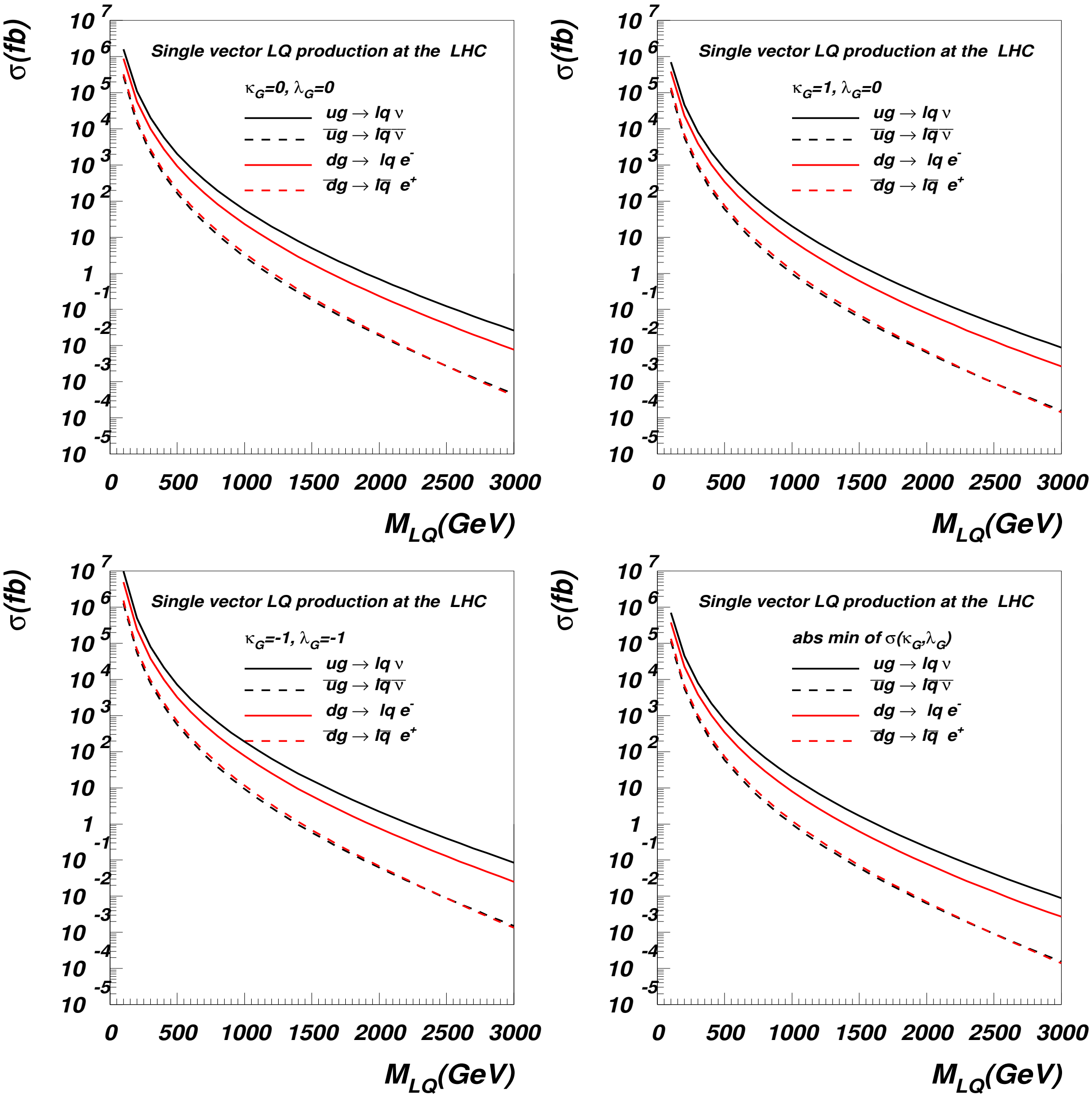

Figure 6: Total cross section of single vector $LQ(VM)$ production as a function of the LQ mass. The cross section of LQ single production depends on its quark content and the value $LQ - \ell - q$ coupling chosen to be $\sqrt{g_{2R}^2 + g_{2L}^2} = \lambda_{\rm eff} = e$. single LQ production in association with the charged lepton is denoted by black curves, while its production in association with neutrino is denoted by red curves. Four choices of (κ, λ) are presented: 1) $\kappa_G = \lambda_G = 0$ — Yang-Mills type coupling (YM); 2) $\kappa_G = 1$, $\lambda_G = 0$ — Minimal coupling (MC); 3) $\kappa_G = -1$, $\lambda_G = -1$ — (MM) case and 4) the case of *absolute minimal cross section* (AM) in which the cross section is minimized with respect to κ_G, λ_G parameters for each value of M_{LQ}.

Vector LQ cross sections are presented in figure 5 and figure 6 for the cases of LQ single and pair production, respectively. We present results for four 'traditional' choices of κ_G and λ_G:

1. $\kappa_G = \lambda_G = 0$, Yang-Mills type coupling (YM) case

2. $\kappa_G = 1$, $\lambda_G = 0$, Minimal coupling (MC) case

3. $\kappa_G = -1$, $\lambda_G = -1$, MM case

4. the case of *absolute minimal cross section* (AM) in which the cross section is minimized with respect to κ_G, λ_G parameters for each value of M_{LQ}.

For AM case, one can establish the absolute conservative limit on the cross section of vector LQ since for each value of M_{LQ} the minimal cross section is defined. One can see again, that the cross section for LQ single production catches up the cross section of pair production at $M_{LQ} \simeq 1\,\text{TeV}$ and starts to dominate at larger LQ masses for the same reason as in scalar LQ production case. One can also notice that the cross section for MC and AM cases are quite close to each other for LQ masses $\leq 1\,\text{TeV}$, e.g. at $M_{LQ} = 1.0\,\text{TeV}$ they are 37.6 fb (MC) and 24.8 fb (AM) for pair vector LQ production and 31.4 fb (MC) and 30.2 fb (AM) for vector LQ single production. Here, we present the sum of the cross sections, $pp \to LQ\ell$ and $pp \to LQ\nu$, of LQ single production processes. However, at higher LQ masses (1.5 − −2 TeV) the cross section for LQ pair production in the AM case could be a factor of 2-3 smaller than for MC case. This happens because the contribution from $gg \to LQ\overline{LQ}$ to the total production cross section (which is similar for MC and AM cases) vanishes for heavy LQ production, while the contribution from $q\bar{q} \to LQ\overline{LQ}$ starts to dominate (it is several times larger for MC, as compared to AM case) in this mass region.

The cross section for YM case is typically a factor of 3-5 higher than the one for MC case. For example, for $M_{LQ} = 1.0\,\text{TeV}$ one has 208 fb and 87.3 fb for LQ single and pair production cross section for YM case. For MM case, the cross section for pair LQs is 1-3 orders of magnitude higher than the one for MC case: $\sigma^{\text{pair}}_{LQ}(MM) = 1760\,\text{fb}$ for $M_{LQ} = 1.0\,\text{TeV}$. The MM cross section for LQ single production is about one order of magnitude higher, as compared to MC case: : $\sigma^{\text{single}}_{LQ}(MM) = 284\,\text{fb}$ for $M_{LQ} = 1.0\,\text{TeV}$.

In table 3, we summarize cross sections for LQ single and pair production for both, vector (VM) and scalar ($S0$) leptoquarks at the LHC. As we mentioned above, the total cross section for any LQ type can be obtained from table 3 by superimposing respective numbers and rescaling them for a chosen value of $LQ - \ell - q$ coupling.

In our study we use the MC set of cross sections (which is not very different from AM case) to establish a conservative limit on the M_{LQ} and λ_{eff} parameters of the model.

4. Simulations and signal versus background analysis

The simulations of leptoquark signal events were performed with CompHEP [19], the CompHEP-PYTHIA interface [25] and PYTHIA6.2 [26] program chain. The cross section values presented in this article were calculated using CTEQ6L parton distribution function (PDF) [27]. PYTHIA was used to account for initial and final state radiation and to perform hadronization and decay of resonances, when it was relevant.

Besides the difference in cross section for vector and scalar LQ production one could expect a difference in angular correlations of vector LQ decay products compared to scalar LQ if the vector LQ is being produced with some polarization. We have found that, indeed, vector LQ is produced with non-trivial polarization at the LHC which is reflected, for instance, in a difference in the angular distribution between the leading p_T electron and jet

M_{LQ} (TeV)	LQ pair production					
	Scalar	Vector (κ, λ)				
		MM $(-1,-1)$	YM $(0,0)$	MC $(1,0)$	AM	(κ, λ)
0.1	1.04E+06	5.05E+11	8.55E+07	3.34E+07	2.31E+07	(0.549, 0.00363)
0.5	3.45E+02	5.23E+05	2.02E+04	4.12E+03	3.31E+03	(1.01, 0.0496)
1.0	4.20E+00	1.76E+03	2.08E+02	3.76E+01	2.48E+01	(1.16, 0.130)
1.5	1.79E-01	4.89E+01	7.84E+00	1.44E+00	7.12E-01	(1.25, 0.198)
2.0	1.19E-02	2.57E+00	4.70E-01	8.96E-02	3.32E-02	(1.30, 0.239)

M_{LQ} (TeV)	LQ single production: $pp(ug) \to LQ\ell$					
	Scalar	Vector (κ, λ)				
		MM $(-1,-1)$	YM $(0,0)$	MC $(1,0)$	AM	(κ, λ)
0.1	5.35E+04	1.12E+07	1.87E+06	8.25E+05	8.15E+05	(0.991, 0.0381)
0.5	1.12E+02	7.80E+03	2.22E+03	8.35E+02	8.20E+02	(1.06, 0.0792)
1.0	4.37E+00	1.97E+02	6.05E+01	2.21E+01	2.10E+01	(1.06, 0.0656)
1.5	4.79E-01	1.66E+01	5.15E+00	1.75E+00	1.74E+00	(1.05, 0.0215)
2.0	1.60E-01	2.29E+00	7.10E-01	2.38E-01	2.37E-01	(1.04, -0.0437)

M_{LQ} (TeV)	LQ single production: $pp(dg) \to LQ\nu$					
	Scalar	Vector (κ, λ)				
		MM $(-1,-1)$	YM $(0,0)$	MC $(1,0)$	AM	(κ, λ)
0.1	3.71E+04	6.55E+06	1.21E+06	5.20E+05	5.15E+05	(1.01, 0.0431)
0.5	6.30E+01	3.93E+03	1.14E+03	4.23E+02	4.15E+02	(1.06, 0.0790)
1.0	2.11E+00	8.70E+01	2.68E+01	9.30E+00	9.20E+00	(1.06, 0.0554)
1.5	2.06E-01	6.60E+00	2.05E+00	6.90E-01	6.90E-01	(1.05, 0.0429)
2.0	3.13E-02	8.25E-01	2.56E-01	8.60E-02	8.55E-02	(1.04, -0.0828)

Table 3: Cross sections (in fb) for LQ single and pair production for vector (VM) and scalar ($S0$) leptoquarks at the LHC. The cross section of LQ single production depends on its quark content and the value of $LQ - \ell - q$ coupling chosen to be $\sqrt{g_{2R}^2 + g_{2L}^2} = \lambda_{\rm eff} = e$. single LQ production in association with a neutrino is presented separately from LQ production in association with a charged lepton. Four choices for (κ, λ) are presented for vector LQ production: 1) $\kappa_G = \lambda_G = 0$ – Yang-Mills type coupling (YM); 2) $\kappa_G = 1$, $\lambda_G = 0$ – Minimal coupling (MC); 3) $\kappa_G = -1$, $\lambda_G = -1$ – (MM) case and 4) the case of *absolute minimal cross section* (AM) in which the cross section is minimized with respect to κ_G, λ_G parameters for each value of M_{LQ}.

shown as an example in figure 7 for LQ single production case. The study of such angular correlation effects is, however, beyond the scope of the present article. The distributions of kinematical characteristics we have chosen in this study are similar for scalar and vector LQ production.

The ATLFAST [28] code has been used to take into account the experimental conditions prevailing at LHC for the ATLAS detector. The detector concept and its physics potential

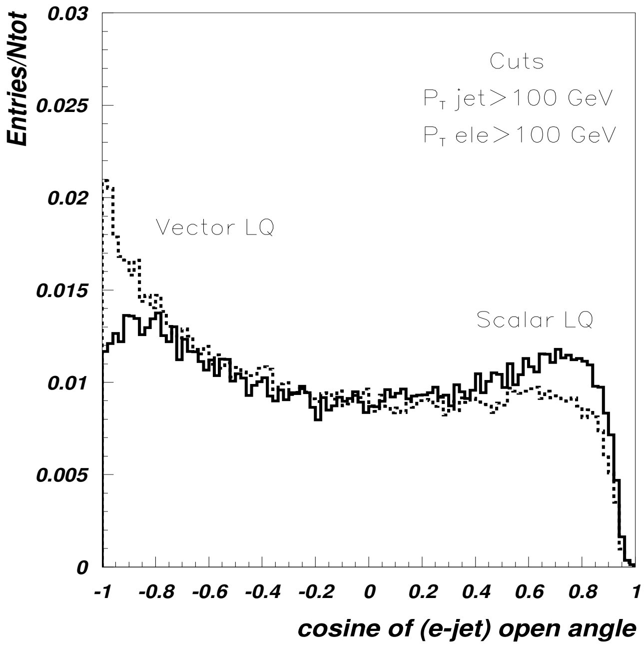

Figure 7: Distributions of the cosine of the open angle between electron and jet in events with a scalar (solid line) and vector (dashed line) $\not{L}Q$ single production.

have been presented in the Technical Proposal [29] and the Technical Design Report [30]. The ATLFAST code for fast detector simulations accounts for most of the detector features: jet reconstruction in the calorimeters, momentum/energy smearing for leptons and photons, magnetic field effects and missing transverse energy. It provides a list of reconstructed jets, isolated leptons and photons. In most cases, the detector-dependent parameters were tuned to values expected for the performance of the ATLAS detector from full simulation.

The electromagnetic calorimeters were used to reconstruct the energy of leptons in cells of dimensions $\Delta\eta \times \Delta\phi = 0.025 \times 0.025$ within the pseudorapidity (η) range $-2.5 < \eta < 2.5$; ϕ is the azimuthal angle. The electromagnetic energy resolution is given by $0.1/\sqrt{E}(GeV) \bigoplus 0.007$ over this pseudorapidity region. The electromagnetic showers are identified as leptons when they lie within a cone of radius $\Delta R = \sqrt{(\Delta\eta)^2 \times (\Delta\phi)^2} = 0.2$ and possess a transverse energy $E_T > 5\,\text{GeV}$. Lepton isolation criteria were applied, requiring a distance $\Delta R > 0.4$ from other clusters and maximum transverse energy deposition, $E_T < 10\,\text{GeV}$, in cells in a cone of radius $\Delta R = 0.2$ around the direction of electron emission.

Jet energies were reconstructed by clustering hadronic calorimeters cells of dimensions $\Delta\eta \times \Delta\phi = 0.1 \times 0.1$ within the pseudorapidity range $-2.5 < \eta < 2.5$. The hadronic energy resolution of the ATLAS detector is parametrized as $0.5/\sqrt{E(GeV)} \oplus 0.03$ over this η region. Hadronic showers are regarded as jets if the deposited transverse energy E_T is greater than $15\,\text{GeV}$ within a cone of radius $\Delta R = 0.4$.

It must be mentioned that standard parametrization in ATLFAST has been used for the electron resolution but detailed studies are needed, using test beam data and GEANT full simulation to validate the extrapolation of the resolution function to electron energies

Process	$t\bar{t}$(Type 1)	$t\bar{t}$ (Type 2)	$Z + jet$	$W + jets$
σ (pb)	6.6	11	665	17.

Table 4: Cross section σ(pb) from PYTHIA for the backgrounds after pre-selection cuts.

in the TeV range.

In this paper, two types of signal event have been studied.

1. *Type 1*$(2l + jets)$ signature, for which $I\!\!Q$ produced singly in association with an electron, decays to an electron and a quark, while each $I\!\!Q$ produced in pair is required to decay to an electron and a quark.

2. *Type 2*$(l + jets + E_T^{\rm miss})$ signature, for which $I\!\!Q$ produced singly in association with a neutrino, decays to an electron and a quark.[1] For $I\!\!Q$ pair production, one $I\!\!Q$ is required to decay into electron and quark, while the other one – to a neutrino and a quark.

Backgrounds of Type 1 signal signature are $Z + jets$ events, where Z decays into two electrons, and $t\bar{t}$ events where both W from the top quark decay into an electron (positron) and a neutrino. For the signal events of Type 2, backgrounds are $W + jets$ events, where W decays into an electron and a neutrino, and $t\bar{t}$ events where one W decays into an electron and neutrino, and the second W decays into jets.

In order to enrich the event statistics in the region of high invariant masses, simulated background events were pre-selected in PYTHIA for hard $2 \to 2$ process with transverse momentum, $\hat{p}_T > 200\,\mathrm{GeV}$ ($100\,\mathrm{GeV}$ for $Z + jet$ events), defined in the rest frame of the hard interaction, followed by the standard initial and final state radiation technique. Top quark pair production and $W + jets$ background events for Type 2 signal events were additionally pre-selected with at least one electron and $\not{E}_T > 100\,\mathrm{GeV}$. Corresponding cross sections for the backgrounds, used for this article, are shown in table 4 for the events, passing pre-selection cuts. Since the signal events would consist of events originated from the single or pair production of leptoquarks, we tried to define a unique set of cuts effective for the background suppression against combined $I\!\!Q$ pair+single signal.

4.1 Type 1 $I\!\!Q$ signal events

Here, we present the analysis of $I\!\!Q$ events of Type 1. The signal signatures consist of at least one jet and two electrons.

Due to their large mass, leptoquarks would produce events with large transverse energy. The scalar sum of transverse momenta of all charged particles in the event, H_T, is presented for single, figure 8 (left), and pair, figure 8 (right), scalar $I\!\!Q$ production. As can be seen, an appropriate choice of a H_T value should suppress the bulk of background events.

The following cuts were used to separate signal from background:

[1]The same signature will be for single $I\!\!Q$ production in association with the electron if $I\!\!Q$ decays into neutrino and quark.

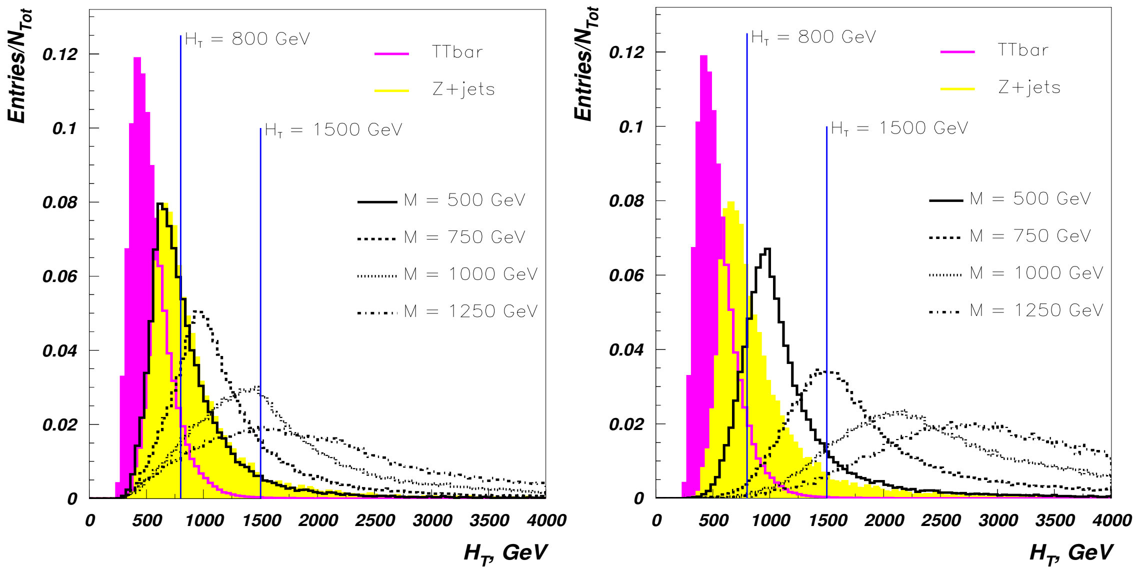

Figure 8: Distribution of the H_T variable (see text) for events of single (left) and pair (right) production of scalar leptoquarks and corresponding backgrounds. All distributions are normalized to unity.

- The transverse momentum of two electrons were required to be at least 90 GeV (100 GeV in the case of $M_{LQ} > 750$ GeV).
- At least one jet was required with minimum transverse momenta of 70 GeV (90 GeV in the case of $M_{LQ} = 750$ GeV and > 100 GeV/c for higher LQ masses).
- The invariant mass of two electrons was required to be larger than 150 GeV in order to veto the dominant $Z + jets$ background.
- Events with at least one b-jet were vetoed to suppress $t\bar{t}$ background.
- The scalar transverse momentum sum of all selected particles in the event, H_T, was required to be at least 800 GeV.

The resulting invariant mass distributions for the electron-jet system are presented in figures 9 for combined single and pair production of leptoquarks of various masses. Signal distributions are presented for scalar (hatched area) and vector leptoquarks. The dashed line shows the pair production contribution to the total signal spectrum. The contribution of the single production to the total spectrum gradually increases with the LQ mass. The cross section for vector leptoquarks corresponds to MC case ($\kappa_G = 1$, $\lambda_G = 0$).

All possible mass combinations between two leading p_T jets and electrons are allowed, which leads to some broadening of the signal distributions for the single production case.

As can be seen from these figures, the $Z + jets$ background is essentially dominant. The pair production of top quarks gives a rather small contribution and can be seen only for the lowest leptoquark mass case studied.

The signal statistical significances are given in table 5. The data are presented for combined (single+LQ pair production) signal efficiencies, with the number of events shown

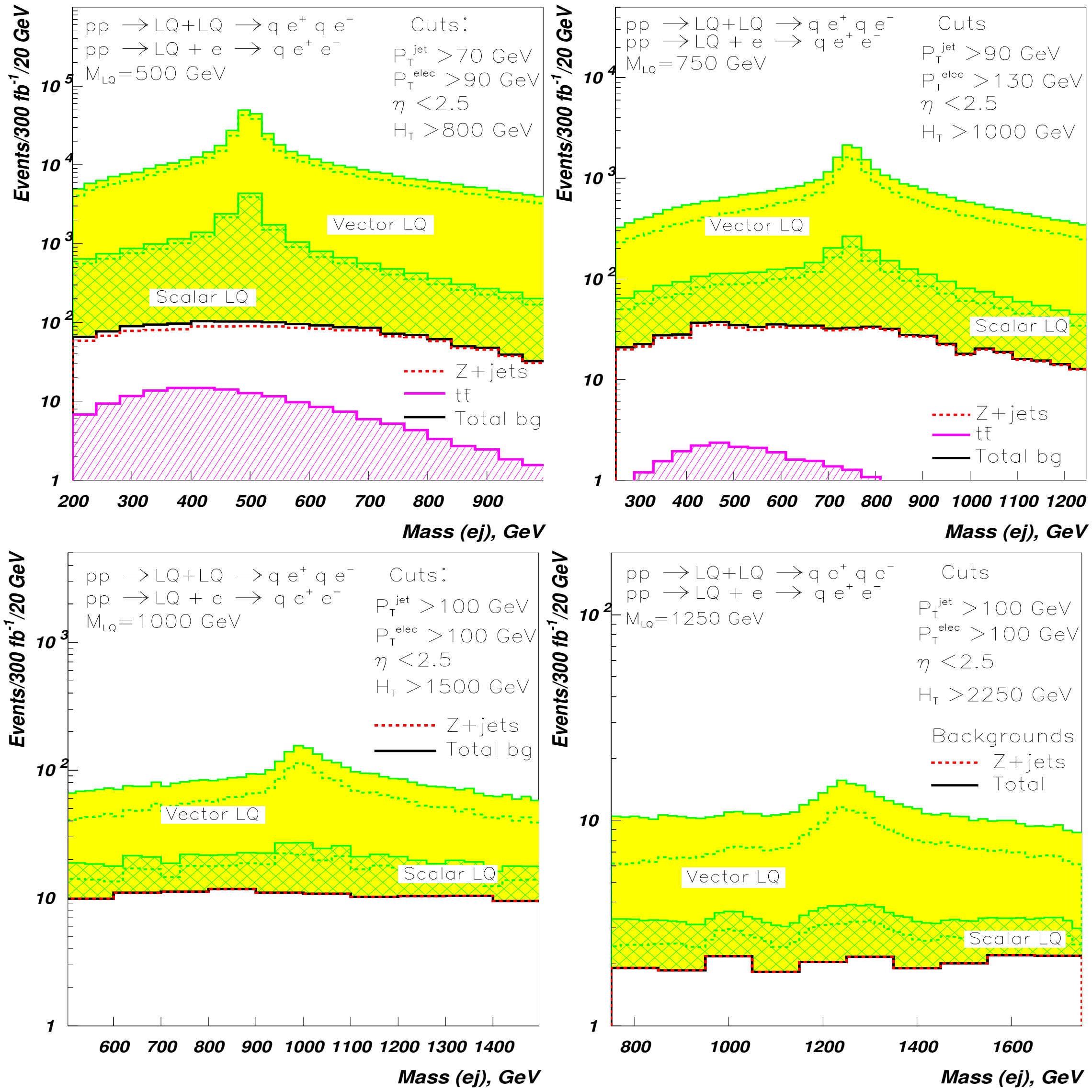

Figure 9: Invariant mass distribution of electron and jet for events of single and pair production of scalar and vector leptoquarks mass 500, 750, 1000 and 1250 GeV for Type 1 signal events.

for the total background and for $\not{L}Q$ single and pair production for different masses of scalar and vector leptoquarks. The data are presented for an integrated luminosity of $L = 300\,\text{fb}^{-1}$.

$I\!\!Q$ Mass (GeV)	Background	Scalar $I\!\!Q$			Vector $I\!\!Q$		
		$I\!\!Q$-Single	$I\!\!Q$-Pair	$S_{\rm tot}/\sqrt{B}$	$I\!\!Q$-Single	$I\!\!Q$-Pair	$S_{\rm tot}/\sqrt{B}$
500	614	1835	14529	660	25907	155374	7316
750	264	335	1033	84	2902	8571	706
1000	132	54	112	14	392	894	112
1250	40	12	17	5	70	140	33
1500	28	4	3	1	16	20	7

Table 5: Number of signal events for $I\!\!Q$ single and pair production versus total background and respective significance $S_{\rm tot}/\sqrt{B}$ for combined signal ($I\!\!Q$ pair + single production). Results are for an integrated luminosity of $L = 300\,{\rm fb}^{-1}$ and Type 1 signal signature.

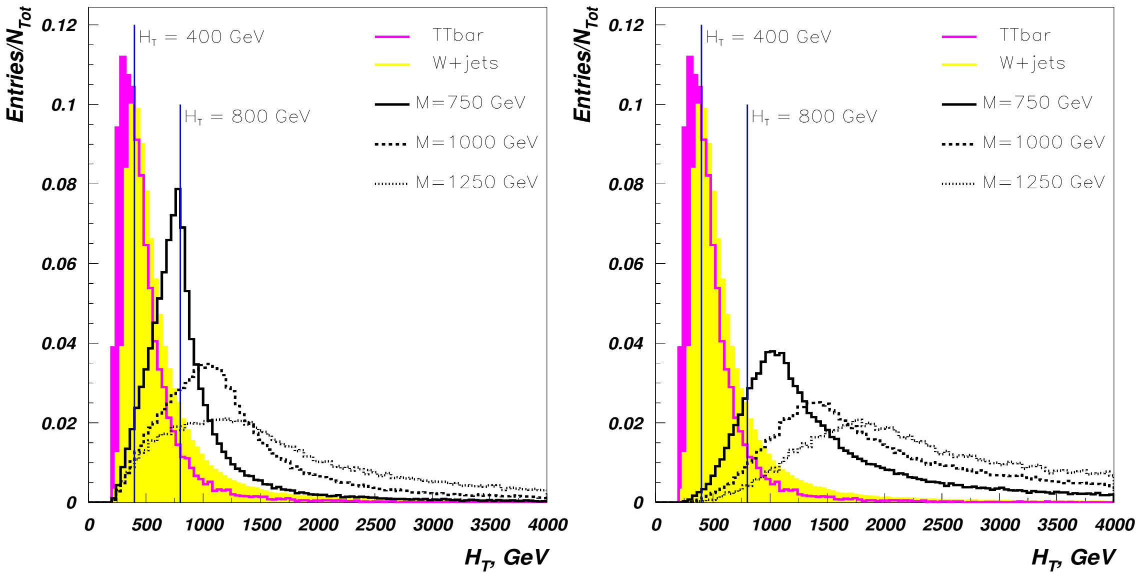

Figure 10: Distribution of H_T variable (see text) for events of single (left) and pair (right) production of leptoquarks and corresponding backgrounds. Decays of LQ include electrons and neutrino. All distributions are normalized to unity.

4.2 Type 2 LQ signal events

In this section we present the analysis of signal events with an electron, jets and a neutrino. The signal signature is at least one jet, electron and missing transverse momenta. The scalar sum of transverse momenta of all charged particles in the event, H_T, is presented for single, figure 10 (left), and pair production, figure 10 (right) of scalar LQ. As can be seen, an appropriate choice of a H_T value again should suppress the bulk of background events. The presence of a neutrino in the LQ signal events of this type, provides a possibility to suppress relevant backgrounds using a missing transverse momentum variable. In figure 11 (right), we plot the orbital (ϕ)-angle difference, $\Delta\phi$, between electron and the missing transverse momentum vector. Distributions are shown for scalar and vector leptoquark decays and corresponding backgrounds. The background spectra reveal the emission of an electron and a neutrino along the same direction, which is reasonable, since in background events those particles are produced in W decays. The signal distributions bear mostly the back-to-back emission feature.

The following set of cuts was worked out to effectively separate the signal from background:

- The transverse momentum of the electron was required to be at least 100 GeV.
- At least one jet was required with a minimum transverse momentum of at least 100 GeV.
- The transverse mass of an electron and the missing transverse momentum vector ($P_T^{\rm miss}$, see figure 12) was required to be larger than 200 GeV in order to veto the dominant $W + jets$ background.

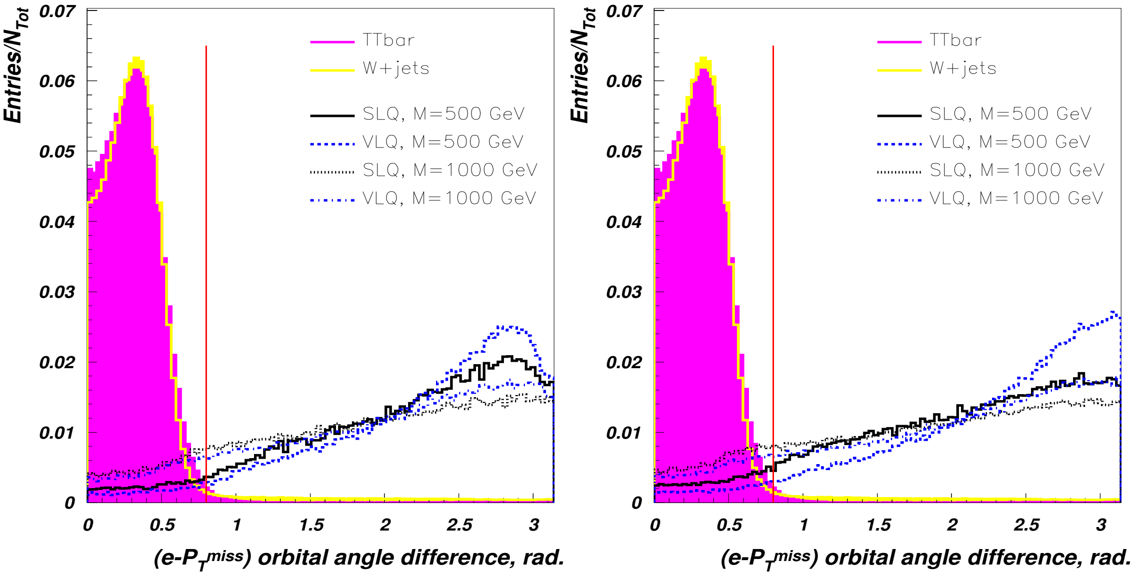

Figure 11: The distribution of the orbital ϕ-angle difference between an electron and the missing transverse momentum vector, $\Delta\phi$, in radians, for signal (scalar and vector LQ) and background $W + jets$ and $t\bar{t}$ events. single (left) and pair (right) LQ production are presented.

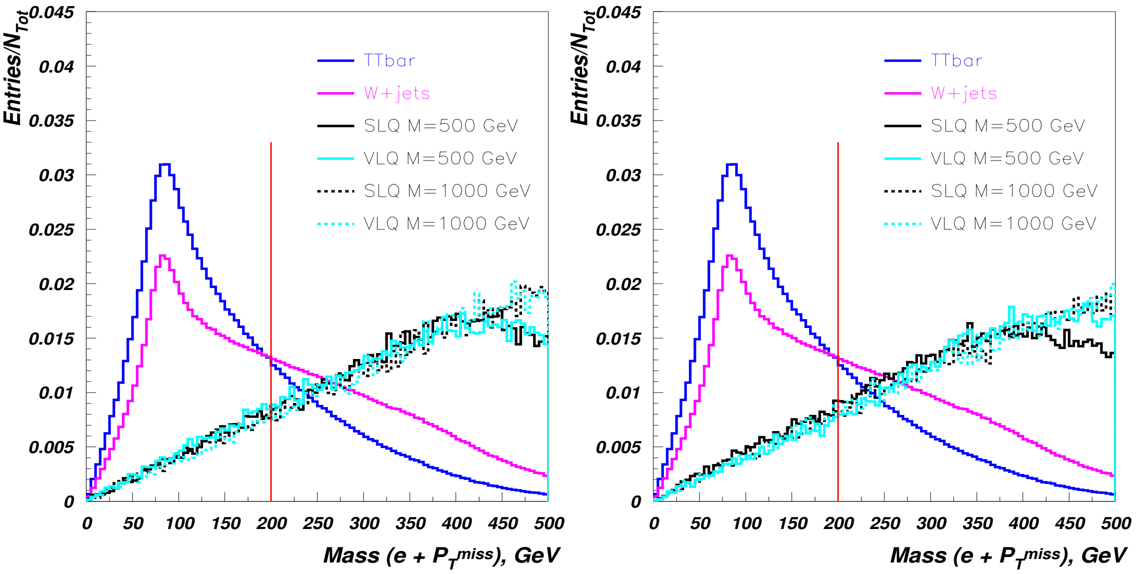

Figure 12: The distribution of the transverse mass of an electron and the $P_T^{\rm miss}$ vector for signal (scalar and vector LQ) and $W+jets$ and $t\bar{t}$ backgrounds. single (left) and pair (right) LQ production are presented.

- Events with at least one b-jet were vetoed to suppress $t\bar{t}$ background.
- The scalar sum of transverse momenta of all selected particles in the event, H_T, was required to be at least 400,(600, 800, 1000, 1200) GeV for LQ masses of 500, (750, 1000, 1250, 1500) GeV, respectively.

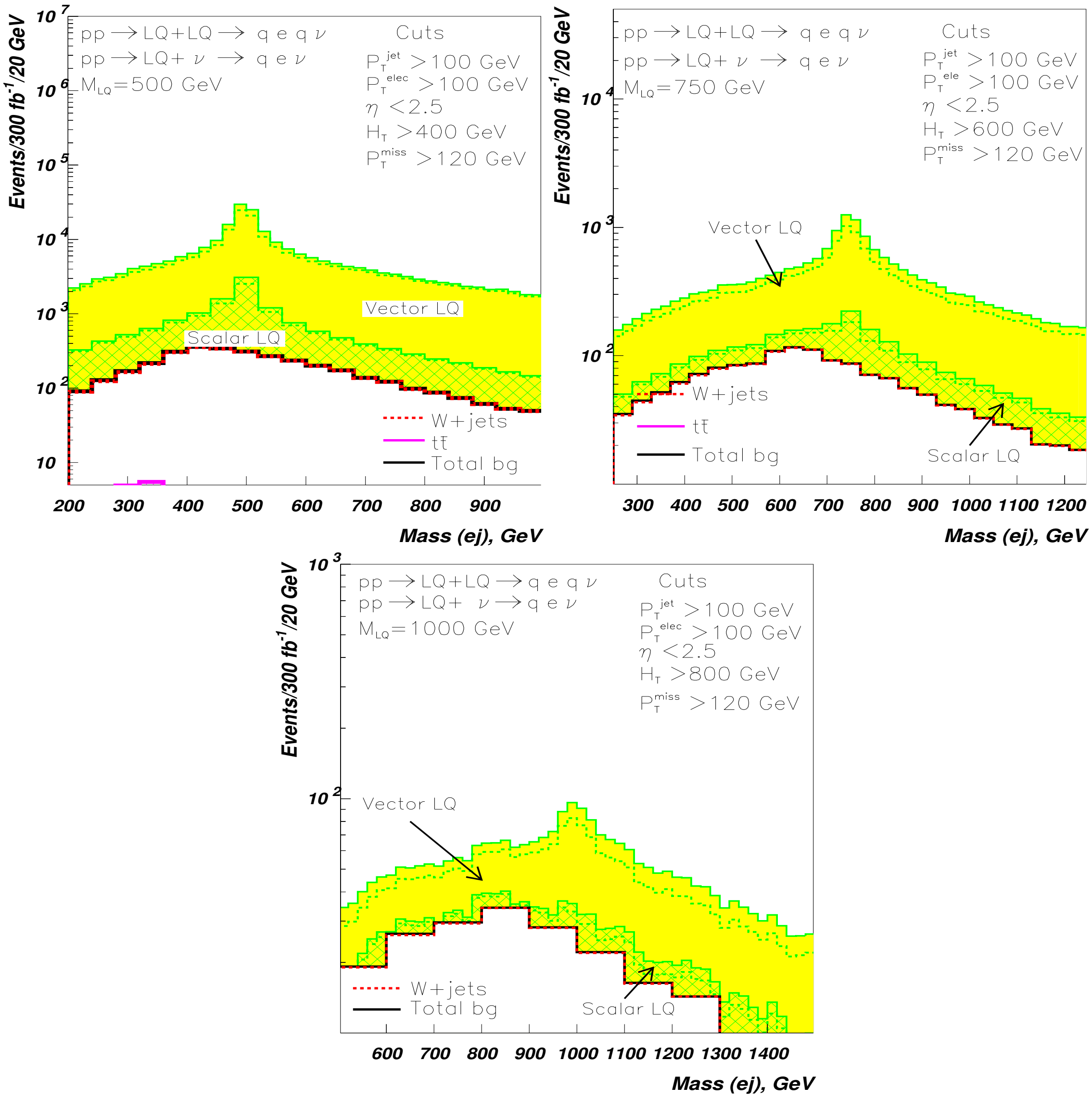

Figure 13: Invariant mass distribution of electron and jet for events of single and pair production of scalar and vector leptoquarks for $m = 500\,\mathrm{GeV}$ (upper left) and $m = 750\,\mathrm{GeV}$ (upper right) and $m = 1000\,\mathrm{GeV}$ (below) for Type 2 signature.

- The orbital angle difference between an electron and the transverse missing momentum vector was required to be greater than 0.8 radians.

While the angular spectra of scalar and vector $\not{L}\!Q$ of 500 GeV mass are quite close to the background spectra in the forward hemisphere, the signal distributions for larger masses allow the separation of the signal from the background. The resulting invariant mass distributions for the electron-jet system of the signal events of Type 2 are presented in figure 13 for the $\not{L}\!Q$ mass of 500 GeV (left side) and 750 GeV (right side). Signal distributions are presented for scalar leptoquarks (hatched area) and vector leptoquarks for the minimal coupling set. The dashed line shows the pair production contribution to the total signal

Mass (GeV)	Background	Scalar LQ			Vector LQ		
		LQ-Single	LQ-Pair	$S_{\text{tot}}/\sqrt{B}$	LQ-Single	LQ-Pair	$S_{\text{tot}}/\sqrt{B}$
500	1850	2093	8383	244	17889	88438	2425
750	674	251	545	31	1229	4953	238
1000	303	33	52	5	135	460	34
1250	149	5	7	1	17	64	7

Table 6: Number of signal events for single and LQ pair production versus total background and respective significance $S_{\text{tot}}/\sqrt{B}$ for combined signal (pair + LQ single production). Results are for an integrated luminosity of $L = 300\,\text{fb}^{-1}$ and Type 2 signature.

spectrum. Similarly to the Type 1 signal events, the contribution of the single production to the total spectrum gradually increases with the LQ mass. The signal statistical significances are reported in table 6 combined for LQ single and pair production for different LQ masses. Table 6 also presents number of events, separately for for LQ single and pair production as well as for background events. The data correspond to an integrated luminosity of $L = 300\,\text{fb}^{-1}$.

4.3 LQ mass reach of LHC

The LQ mass reach of LHC is shown in figure 14 for combined single and LQ pair production processes and two types of signal signatures. The results for scalar and vector LQ are presented separately. The data are presented for an integrated luminosity of $L = 300\,\text{fb}^{-1}$. One can see that scalar leptoquarks can be accessible at LHC up to masses $\lesssim 1.2\,\text{TeV}$ while vector LQ for MC case can be discovered for masses $\lesssim 1.5\,\text{TeV}$. LHC can exclude LQ at 95% CL with masses about 200 GeV above 5σ discovery LQ limit, i.e. with masses $\lesssim 1.4\,\text{TeV}$ and $\lesssim 1.7\,\text{TeV}$ for scalar and vector (MC) LQ, respectively.

Let us remind, that we have chosen $LQ - l - q$ coupling $\lambda_{\text{eff}} = e$ and contribution from LQ single production rescales quadratically with this coupling. For other values of λ_{eff}, the new LHC reach can be easily found by using LHC reach tables 5 and 6. One can see that Type 1 signature ($2\ell + jets$) looks more promising compared to Type 2 events ($2\ell + jets + \not{E}_T$).

One should notice that, for the chosen λ_{eff}, the contribution from LQ single production is 30-50% to the total number of signal events for the LQ mass at the discovery limit. Therefore, LQ single and pair production should be studied together at the LHC.[2] The complementarity of single and pair LQ channels is clearly illustrated in our final figure 14, where we present scalar and vector leptoquark mass reach of the LHC in the ($M_{LQ} - \lambda_{\text{eff}}$) plane. For example, for $\lambda_{\text{eff}} = 1$, LQ single production allows the extension of LHC reach for M_{LQ} by about 400 GeV!

[2]Eventually, the case of single production of LQ of the second and third generations is qualitatively different. In this case only pair LQ would give the major contribution to the signal rates, unless λ_{eff} is too large (which might be not allowed by other experimental constraints) to enhance LQ single production, suppressed due to initial sea-quarks PDFs.

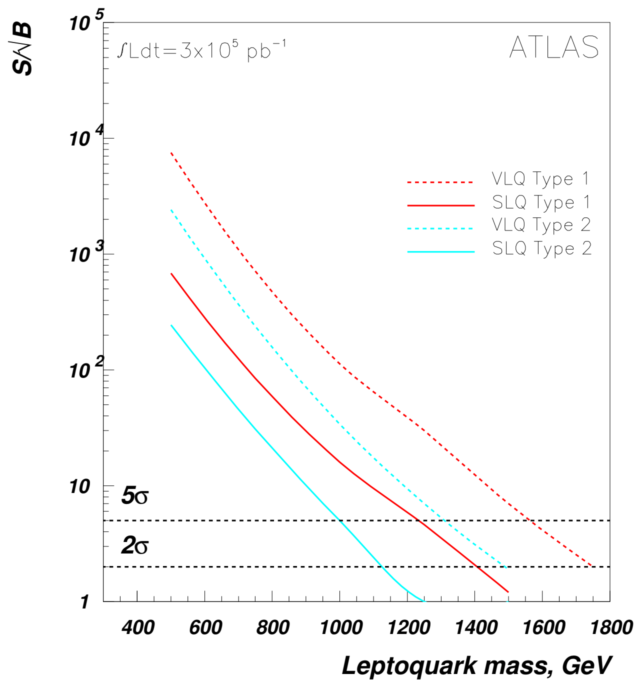

Figure 14: Leptoquark mass reach of the LHC at 5σ level for Type 1 and Type 2 signal signatures for scalar (solid line) and vector (dashed line) LQ for an integrated luminosity of $L = 300\,\mathrm{fb}^{-1}$. For vector LQ, the MC choice has been selected. The contributions of single and pair LQ signal are combined.

5. Conclusions

In this paper, we present a new detailed study of LQ production and decay at LHC at the level of detector simulation.

We treated LQ single and pair production together and have worked out a set of kinematical cuts to maximize significance for combined single and pair production events.

It was shown, that combination of signatures from LQ single and pair production not only significantly increases the LHC reach, but also allows us to give the correct signal interpretation. Our results are summarized in tables 5 and 6 and figures 14 and 15. In particular, the LHC can discover LQ with a mass up to 1.2 TeV and 1.5 TeV for the case of scalar and vector LQ, respectively (for $\lambda_{\text{eff}} = e$), and LQ single production contributes 30-50% to the total signal rate.

In this work, the most general form of scalar and vector LQ interactions with quarks and gluons has been implemented into CalcHEP/CompHEP packages, which was one of the primary aspects of this study.

Acknowledgments

A.B. grateful to Oscar Eboli, C.P. Yuan, Jon Pumplin, Thomas Nunnemann and John R. Smith for stimulating discussions. C.L. and R.M. thank NSERC/Canada for their support. DOE support is also acknowledged. This work has been performed within the

JHEP09(2005)005

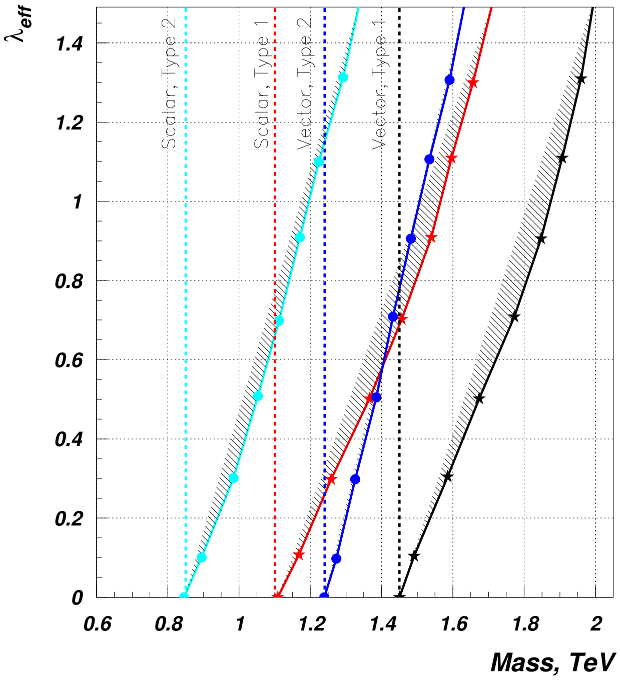

Figure 15: Scalar and vector leptoquark mass reach of the LHC for $(M_{LQ} - -\lambda)$ plane for LQ pair production (dashed line) and for combined LQ single and pair production (solid line). Type 1 signal reach contour is denoted by stars while Type 2 signal reach contour is marked by solid dots.

ATLAS Collaboration with the help of the simulation framework and tools which are the result of the collaboration-wide efforts.

References

[1] For reviews and references see e.g. S. Dimopoulos, S. A. Raby and F. Wilczek, *Unification of couplings*, *Phys. Today* **44N10** (1991) 25;
PARTICLE DATA GROUP, K. Hagiwara et al., *Review of particle physics*, *Phys. Rev.* **D 66** (2002) 010001.

[2] See e.g. J.L. Hewett, *Single squark production at hera via R-parity violating interactions*, MAD-PH-598, contribution to Proc. of 1990 *Summer study on high energy physics - research directions for the decade*, Snowmass, CO, Jun 25–Jul 13, 1990;
H.K. Dreiner and G.G. Ross, *R-parity violation at hadron colliders*, *Nucl. Phys.* **B 365** (1991) 597;
J. Butterworth and H.K. Dreiner, *R-parity violation at HERA*, *Nucl. Phys.* **B 397** (1993) 3 [hep-ph/9211204];
J.C. Romao, C.A. Santos and J.W.F. Valle, *How to spontaneously break R-parity*, *Phys. Lett.* **B 288** (1992) 311.

[3] B. Schrempp and F. Schrempp, *Light leptoquarks*, *Phys. Lett.* **B 153** (1985) 101.

[4] ZEUS collaboration, S. Chekanov et al., *A search for resonance decays to lepton + jet at HERA and limits on leptoquarks*, *Phys. Rev.* **D 68** (2003) 052004 [hep-ex/0304008];
H1 collaboration, C. Adloff et al., *A search for leptoquark bosons in e-p collisions at HERA*, *Phys. Lett.* **B 523** (2001) 234 [hep-ex/0107038];

H1 collaboration, C. Adloff et al., *Search for compositeness, leptoquarks and large extra dimensions in e q contact interactions at HERA*, *Phys. Lett.* **B 479** (2000) 358 [hep-ex/0003002];
H1 collaboration, U.F. Katz, *Search for excited fermions and leptoquarks at HERA*, hep-ex/9910012;
H1 collaboration, C. Adloff et al., *A search for leptoquark bosons and lepton flavor violation in e^+p collisions at HERA*, *Eur. Phys. J.* **C 11** (1999) 447 [hep-ex/9907002].

[5] D0 collaboration, V.M. Abazov et al., *Search for leptoquark pairs decaying to $\nu\nu$+ jets in $p\bar{p}$ collisions at $\sqrt{s} = 1.8$ TeV*, *Phys. Rev. Lett.* **88** (2002) 191801 [hep-ex/0111047];
D0 collaboration, V.M. Abazov et al., *Search for first-generation scalar and vector leptoquarks*, *Phys. Rev.* **D 64** (2001) 092004 [hep-ex/0105072];
CDF collaboration, R. Haas, *Search for second and third generation leptoquarks at cdf*, *Int. J. Mod. Phys.* **A 16S1B** (2001) 876 [hep-ex/0010064];
CDF collaboration, F. Abe et al., *Search for third-generation leptoquarks from technicolor models in $p\bar{p}$ collisions at $\sqrt{s} = 1.8$ TeV*, *Phys. Rev. Lett.* **82** (1999) 3206; *Search for first generation leptoquark pair production in $p\bar{p}$ collisions at $\sqrt{s} = 1.8$ TeV*, *Phys. Rev. Lett.* **79** (1997) 4327 [hep-ex/9708017].

[6] B. Dion, L. Marleau, G. Simon and M. de Montigny, *Scalar leptoquark pair production at the cern LHC: signal and backgrounds*, *Eur. Phys. J.* **C 2** (1998) 497 [hep-ph/9701285].

[7] O.J.P. Eboli, R. Zukanovich Funchal and T.L. Lungov, *Signal and backgrounds for leptoquarks at the cern LHC*, *Phys. Rev.* **D 57** (1998) 1715 [hep-ph/9709319].

[8] J.E. Cieza Montalvo, O.J.P. Eboli, M.B. Magro and P.G. Mercadante, *Signal and backgrounds for the single production of scalar and vector leptoquarks at the LHC*, *Phys. Rev.* **D 58** (1998) 095001 [hep-ph/9805472].

[9] A. Belyaev, O.J.P. Eboli, R. Zukanovich Funchal and T.L. Lungov, *Signal and backgrounds for leptoquarks at the LHC, II. Vector leptoquarks*, *Phys. Rev.* **D 59** (1999) 075007 [hep-ph/9811254].

[10] S. Abdullin and F. Charles, *Study of leptoquark pair production at the LHC with the CMS detector*, *Phys. Lett.* **B 464** (1999) 223 [hep-ph/9905396].

[11] M. Kramer, T. Plehn, M. Spira and P.M. Zerwas, *Pair production of scalar leptoquarks at the Tevatron*, *Phys. Rev. Lett.* **79** (1997) 341 [hep-ph/9704322].

[12] A. Alves, O. Eboli and T. Plehn, *Stop lepton associated production at hadron colliders*, *Phys. Lett.* **B 558** (2003) 165 [hep-ph/0211441].

[13] M. Kramer, T. Plehn, M. Spira and P.M. Zerwas, *Pair production of scalar leptoquarks at the LHC*, *Phys. Rev.* **D 71** (2005) 057503 [hep-ph/0411038].

[14] J.L. Hewett and S. Pakvasa, *Leptoquark production in hadron colliders*, *Phys. Rev.* **D 37** (1988) 3165.

[15] O.J.P. Eboli and A.V. Olinto, *Composite leptoquarks in hadronic colliders*, *Phys. Rev.* **D 38** (1988) 3461.

[16] B. Dion, L. Marleau and G. Simon, *Leptoquark pair production at the fermilab Tevatron: signal and backgrounds*, *Phys. Rev.* **D 56** (1997) 479 [hep-ph/9610397].

[17] O.J.P. Eboli and T.L. Lungov, *Single production of leptoquarks at the Tevatron*, *Phys. Rev.* **D 61** (2000) 075015 [hep-ph/9911292].

[18] A. Pukhov, *CalcHEP 3.2: MSSM, structure functions, event generation, batchs and generation of matrix elements for other packages*, hep-ph/0412191.

[19] A. Pukhov et al., *Comphep: a package for evaluation of feynman diagrams and integration over multi-particle phase space. User's manual for version 33*, hep-ph/9908288;
CompHEP collaboration, E. Boos et al., *CompHEP 4.4: automatic computations from lagrangians to events*, *Nucl. Instrum. Meth.* **A534** (2004) 250 [hep-ph/0403113].

[20] W. Buchmuller, R. Ruckl and D. Wyler, *Leptoquarks in lepton quark collisions*, *Phys. Lett.* **B 191** (1987) 442.

[21] J. Blumlein and R. Ruckl, *Production of scalar and vector leptoquarks in* e^+e^- *annihilation*, *Phys. Lett.* **B 304** (1993) 337.

[22] J. Blumlein, E. Boos and A. Kryukov, *Leptoquark pair production in hadronic interactions*, *Z. Physik* **C 76** (1997) 137 [hep-ph/9610408].

[23] P. Cvitanovic, *Group theory for feynman diagrams in nonabelian gauge theories: exceptional groups*, *Phys. Rev.* **D 14** (1976) 1536.

[24] *LQ* models can be downloaded from
http://hep.pa.msu.edu/belyaev/public/projects/lq/models/lq_calc.zip, and at http://hep.pa.msu.edu/belyaev/public/projects/lq/models/lq_comp.zip for CalcHEP and CompHEP, respectively.

[25] A.S. Belyaev et al., *CompHEP-PYTHIA interface: integrated package for the collision events generation based on exact matrix elements*, hep-ph/0101232.

[26] T. Sjostrand, L. Lonnblad and S. Mrenna, *PYTHIA 6.2: physics and manual*, hep-ph/0108264;
T. Sjostrand, *High-energy physics event generation with PYTHIA 5.7 and JETSET 7.4*, *Comput. Phys. Commun.* **82** (1994) 74.

[27] J. Pumplin et al., *New generation of parton distributions with uncertainties from global QCD analysis*, *JHEP* **07** (2002) 012 [hep-ph/0201195].

[28] E. Richter-Was, D. Froidevaux and L. Poggioli: ATLAS Note PHYS-98-131 (1998).

[29] ATLAS collaboration, *Technical proposal*, report no. CERN/LHCC/94-43, 1994.

[30] ATLAS Detector and Physics Performance Technical Design
Report. CERN/LHCC/99-14/15, 1999.

JHEP09(2005)005